Investigations into the nature of the pomeron

Mohammad Badrul Barl

INVESTIGATIONS INTO THE NATURE OF THE POMERON

By

Mohammad Badrul Bari

A thesis presented for the degree of Doctor of Philosophy
of the University of Durham

June 1971

Mathematics Department
University of Durham
England.

PREFACE

The work presented in this thesis was carried out in the Department of Mathematics, University of Durham and the Institute of Physics, University of Islamabad, under the supervision of Professor E.J.Squires. The author expresses his highest appreciation and sincere gratitude to Professor Squires for continuous guidance, encouragement and help. Special thanks are also due to Dr. M.S.K.Razmi, who has partially supervised the work, while the author was in the University of Islamabad.

Except where stated in the text, the work described is original and has not been submitted in this or any other University for the award of a degree. The thesis is based principally on three papers. The author is grateful to Dr. M.S.K.Razmi, Dr. K. Ahmad and Dr. Anis Alam for their permission to include the joint work in this thesis.

The author wishes to thank the Pakistan Atomic Energy Commission for the grant of the Colombo plan fellowship in Britain during the course of his studies.

CONTENTS

ABSTRACT

We investigate the nature of the Pomeranchukon (Pomeron P) singularity in the complex angular momentum plane. To distinguish between simple pole and branch point, we establish and test the factorization rule when Pomeron is exchanged in three particle final states. Further we predict results on the polarization states of resonances when definite parity for Pomeron-pole and mixtures of parities for Pomeron-cut is exchanged. To make comparison of the Pomeron trajectory with other low-lying meson trajectories, we also establish a factorization test for the Rho trajectory and compare it with experimental results.

In Chapter I, we give a general review of Regge-pole theory and also show what difficulties we have with the Pomeron trajectory as compared to other ordinary trajectories. This chapter lays the ground work, explains the problem, and serves as a motivation for the work which was undertaken.

In Chapter II, factorization test for the Pomeron is suggested for reactions with three particle in the final states. It is applied to the available experimental data on $\pi N \to \pi\pi N$ and $NN \to \pi NN$ and is found to be satisfied reasonably well. This gives one evidence that Pomeron is a simple pole.

In Chapter III, we establish a direct test of factorization for the Rho and show from the experimental data, that there is a significant failure of the factorization and also mixture of parities is exchanged in the Rho dominated reactions. It is suggested that cuts play an important part at high energy and indication exists that the Rho particle is a parity doublet.

In Chapter IV, parity test suggested by Gribov is applied to several Pomeron dominated reactions in the high energy production of single baryon or meson resonances. Wherever the experimental data is available, it has been used to compute the relative magnitudes of the residue functions for different helicity states of the Pomeron exchange. Definite predictions on the spin space density matrix elements of the resonances are made for the pole and the cut separately. Suggestions are made to carry out experiments on the decay of unstable particles to check the consistency of our results.

In Chapter V, we conclude by giving a brief review of the present status of the Pomeron trajectory.

CHAPTER I

Introduction and Basic Concept of Regge-pole Theory

1. Regge-pole Model

The idea of analytically continuing the angular momentum to complex values (J-plane) goes back to the work of Watson and Sommerfeld[1]. The subject had achieved success in high energy physics since 1959 when Regge[2] demonstrated the usefulness of considering the analytic properties of a non-relativistic scattering amplitude in the J-plane. Soon afterwards this idea was applied to relativistic scattering of elementary particles by Chew and Frautschi and by Gribov and Pomeranchuk[3]. The theory attempts to describe the direct channel reaction in terms of the analytic properties of the crossed channel amplitudes as a function of the cross channel angular momentum. In this section we briefly explain the mathematical concept and also introduce the notation, which we shall use in the following chapters.

Consider the direct channel (s-channel) process $a+b \rightarrow c+d$ and let it be described by the amplitude $f^s(s, \theta_s)$ where

$$s = (\text{centre of mass energy})^2$$

$$\theta_s = \text{scattering angle in c.m.}$$

Consider also the crossed channel (t-channel) process $a+\bar{c} \rightarrow \bar{b}+d$ (where bars indicate the corresponding anti-particles) and described by the process $f^t(t, \theta_t)$;

where $$t = (\text{c.m. energy})^2$$

$$\theta_t = \text{scattering angle in c.m.}$$

The result of Regge on potential scattering for the t-channel process in the limit $\cos \theta_t \to \infty$

$$f^t(t, \theta_t) \underset{\cos \theta_t \to \infty}{\to} \sum_i \frac{\beta_i(t)}{\sin \pi\alpha_i(t)} (\cos \theta_t)^{\alpha_i(t)}$$

where $\alpha_i(t)$ are trajectory functions associated with the Regge-poles and $\beta_i(t)$ are residue functions, and the sum runs over t-channel Regge-poles. The relativistic generalization of the above formula is

$$f^t(t, \theta_t) \underset{\cos \theta_t \to \infty}{\to} \sum_i \xi_i(t)\, \beta_i(t)\, (\cos \theta_t)^{\alpha_i(t)}$$

where $\xi_i(t)$ is called the signature factor given by

$$\xi_i(t) = \frac{1 + \tau e^{-i\pi\alpha_i(t)}}{\sin \pi\alpha_i(t)}$$

where $\tau = \pm 1$ is the "J-parity" or signature, and has to be introduced in relativistic scattering due to the direct and exchange forces. The functions $\alpha_i(t)$ are called Regge trajectories, and describe the family of particles, since a value of t such that $\alpha_i(t)$ is a non-negative integer is a pole of the amplitude and hence a particle.

There is then an important and most powerful tool of crossing symmetry. For spinless particles $f^s(s, \theta_s) = f^t(t, \theta_t)$. It means that if the function f is analytically continued from one physical region to the other (they do not overlap), then both the processes are described by the same function. Since

$$\cos \theta_t = -1 + \frac{2s}{4m^2 - t}$$

where $t = -(\text{momentum transfer})^2$ in s-channel, therefore the region of high energy $s \gg 2m^2$ and small momentum transfer $|t| < 4m^2$ in direct channel corresponds to having $\cos \theta_t \to \infty$. Using the Regge-asymptotic form and the crossing symmetry, one gets,

$$f(s, \theta_s) \underset{s\to\infty}{\to} \sum_i \xi_i(t)\, \beta_i(t) \left(\frac{s}{s_o}\right)^{\alpha_i(t)} \qquad (1.1)$$

valid for $s \gg 2m^2$ and $|t| < 4m^2$, where s_o is a scaling constant. This is the most far reaching result of the Regge theory. The asymptotic behaviour in $\cos \theta$ of one reaction here gives the observable high energy limit of the reaction corresponding to the crossed channel. Further this crossed-channel theory is very desirable because experimentally high energy reactions are characterized by a definite correlation between the peaking (or lack of it) of a reaction in the forward or backward direction, and the existence (or lack of it) of particles with quantum numbers exchanged in the respective crossed-channel.

At asymptotic energies, a reaction will ultimately be dominated by the single trajectory with definite quantum numbers; Isospin (T), Strangeness (S), C-Parity (C), Parity (P), and variable spin $\alpha(t)$. Let this leading trajectory be $\alpha_L(t)$, then (1.1) reduced to

$$f(s, \theta_s) \underset{s\to\infty}{\to} \beta_L(t)\, \frac{1 + \tau e^{-i\pi\alpha_L(t)}}{\sin \pi\alpha_L(t)} \left(\frac{s}{s_o}\right)^{\alpha_L(t)} .$$

This gives the differential cross-section

$$\frac{d\sigma}{dt} \underset{s\to\infty}{\to} \beta_L(t) \left(\frac{s}{s_o}\right)^{2\alpha_L(t)-2}$$

For fixed t, therefore, the differential cross-section of all reactions with the same exchange of quantum numbers will have the same power behaviour.

Further, to make contact with experiments, we have the optical theorem, which relates the total cross-section with the imaginary part of the elastic scattering amplitude in the forward direction (t = 0),

$$\sigma_{tot}(s) \approx \frac{1}{s} \text{Im } f(s,0).$$

So far, we have taken a very naive picture of having simple poles as in potential theory. But as we shall see that in strong interaction dynamics, which is governed by J-plane singularities, these singularities may be poles, cuts or other essential singularities. Unfortunately at present, there exists no reliable method for computing theoretically the strength of cuts or essential singularity contributions.

2. Diffraction Scattering

The scattering in which the vacuum quantum numbers (Baryon no. = hypercharge = T spin = 0) can be exchanged in the t-channel is called Diffraction scattering. All elastic scattering are of diffractive nature and any two-body inelastic reaction $A + B \rightarrow A' + B'$ in which A' and/or B' have the same internal quantum numbers as A and/or B, would look like diffraction (called the diffraction dissociation). Similarly, in many-body reactions if the final particles can be combined in such a way that the internal quantum numbers of the group of final particles are the same as that of initial particles, then vacuum quantum numbers can be exchanged. See figure No. 1 below.

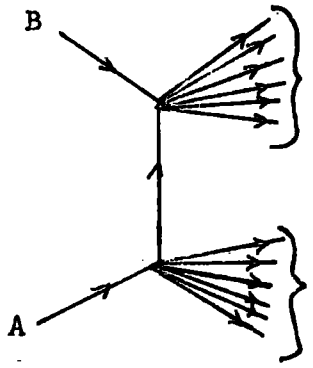

Internal quantum numbers as B.

Internal quantum numbers as A.

Figure 1

On the contrary, any reaction, for example, $k^-p \rightarrow \pi^-\pi^+\Lambda$, cannot be of diffractive type since none of the two particles in the final state can be combined to give the same internal quantum numbers as the initial particles.

3. Froissort bound

It was proved by Froissort[5] that for the scattering of scalar particles the total cross-section can at most behave like $(\log s)^2$ as s tends to infinity. This bound on the scattering amplitude with the help of the optical theorem (unitarity) would imply that $\alpha(0) \leq 1$ for all trajectories. We shall see in the following section that this bound coupled with the constancy of total cross-sections would lead, at very high energy, to the appealing suggestion that forces are as strong as possible if $\alpha(0) = 1$.

4. Pomeron Trajectory

Pomeranchuk in 1958[6] has conjectured two theorems about the high energy limits of total cross-sections, namely:

(i) $\sigma_{ab} \rightarrow \sigma_{a\bar{b}}$ as $s \rightarrow \infty$,

where a is any particle target and b and $\bar{b}$ are particle and anti-particle beams.

(ii) $\sigma_{ab}^{T} \rightarrow \sigma_{ab}^{T'}$ as $s \rightarrow \infty$,

where σ_{ab}^{T} and $\sigma_{ab}^{T'}$ are the total cross-sections for any collision (a,b) in the isotopic spin channels T and T' respectively. The first theorem was based on dispersion relations and the assumption of a finite radius of interaction, which implies that total cross-sections approach constants at high energy. This theorem has since been refined by a number of authors and established under much wider conditions. To explain this feature of apparent constancy of total cross-sections as a function of energy, a trajectory which is called the Pomeranchukon or Pomeron trajectory P, is postulated. From constant total cross-sections, the optical theorem coupled with the Froissort bound demands that $\alpha_p(0) = 1$.

Since the nature of the Pomeron trajectory is the subject of our thesis, we shall only describe in this section a few facts which are fully established. In the last chapter, we shall review the details of the present status of the Pomeron trajectory.

Firstly the quantum numbers of the Pomeron are that of vacuum implying that Pomeron exchange in the t-channel is consistent with diffraction scattering. This can be seen as follows.

Since many elastic amplitudes involve a two-pion vertex $P = +1$ and $G = +$, the signature τ is positive. (In this section, we shall also give two other convincing reasons for the Pomeron to have a positive signature). The second theorem implies that cross-sections

in the limit of high energy are independent of isospin. This means that Pomeron has zero isospin. This means that Pomeron has zero isospin. From the first theorem of Pomeranchuk, applying line reversal, one can show that Pomeron must have positive charge conjugation. This also follows from T = 0 and G = +ve, or from the fact that only mesons with C = +ve contribute to spin average total cross-section.

We give two more reasons to establish that the Pomeron must have positive signature. Firstly, the signature factor can be written as

$$\xi(t) = \begin{cases} \dfrac{1}{\sin(\pi\alpha(t))/2}\left[\exp\left(-i\,\dfrac{\pi\alpha(t)}{2}\right)\right] & \text{for } \tau = +ve \\ \dfrac{1}{\cos(\pi\alpha(t))/2}\left[\exp\left(-i\,\dfrac{\pi\alpha(t)}{2}\right)\right] & \text{for } \tau = -ve \end{cases}$$

If τ = -ve, then $\cos\dfrac{\pi\alpha_p(t)}{2} = 0$; $\xi(t)$ would have a pole at $t = 0$. To avoid this one has to assume that the signature is positive. The second motivation is more convincing. The Pomeranchuk theorem is

$$\sigma_{total}(ab) = \sigma_{total}(\bar{a}b)$$

The t-channel reaction of the left hand side and the right hand side are respectively $a\bar{a} \to \bar{b}b$, and $\bar{a}a \to \bar{b}b$. Now θ_t in the t-channel c.m. in the first reaction, is the angle between a and b and in the second the angle between $\bar{a}$ and b. Since a and $\bar{a}$ are in the centre of mass system, therefore $\cos(\theta_t)$ changes to $-\cos(\theta_t)$ in going from reaction $a\bar{a} \to \bar{b}b$ to $\bar{a}a \to \bar{b}b$. We know the positive signature amplitude is symmetric as a function of $\cos(\theta_t)$, since the contribution of such a Regge-pole to ab and $\bar{a}b$ elastic scattering is the same. Hence only a positive signature Pomeron trajectory can account for the equality of $\sigma_{tot}(ab)$ and $\sigma_{tot}(\bar{a}b)$.

5. Comparison of the Pomeron trajectory with other trajectories

One of the most far reaching consequences of Regge theory is the classification of particles, that all known particles and resonances could be grouped into families, each family being associated with a given Regge trajectory, and consisting of several members differing only in the spin quantum numbers by alternate integer or half-integer. The square of the mass of the particle of spin J would be the value of t for which real part of $\alpha(t)$ is equal to J.

Chew and Frauchtshi, making simplest possible assumptions, drew straight lines representing $\alpha(t)$, joining particles with the same internal quantum numbers and differing by two units of spin and deduced that the slope of the trajectories ρ, π, w, A_2, N ... are equal to

$$\frac{d\alpha(t)}{dt} = \alpha'(t) \approx 1(\text{Gev/c})^{-2} .$$

All these trajectories are now regarded as reasonably well established, but doubts exist for the Pomeron trajectory.

For example, if the slope of the Pomeron trajectory is similar to that of other leading trajectories, there should be an indefinitely continuing shrinkage, as the energy increases, in forward peak widths for all reactions, both elastic and inelastic. More precisely, if $\alpha_p'(0)$ is the Pomeron trajectory slope at $t = 0$ and h is the peak width in $|t|$, then for all reactions with the Pomeron exchange the inverse peak width is predicted to behave as

$$h^{-1} \underset{s\to\infty}{\to} \text{constant} + 2\alpha_p'(0) \log s$$

where s is the square of the total energy. Unfortunately this shrinkage is slow and difficult to observe. For example, in the range

of lab. energies between 10 and 30 Gev a typical value of the inverse width h^{-1} is about 10 $(Gev)^{-1}$. If $\alpha_p'(0)$ is 1 $(Gev)^{-2}$, as is true for other leading trajectories, then the peak width is predicted by the above formula to decrease by only 20%, where s increases by a factor 3. For lab. energies below 100 Gev, variations of such an order of magnitude in the shape of the forward peak can easily be produced by trajectories lying below the Pomeron.

Another long standing difficulty with the interpretation of the Pomeron as a Regge-pole has been the apparent absence of a $J^P = 2^+$, $T^G = 0^+$ particle on the trajectory. If we take the recent experimental data from Serpukhov[7], which show a significant shrinkage in the diffraction peak in pp scattering, then the Regge fit yields a value of 0.4 for the slope of the Pomeron trajectory. Therefore, if the Pomeron trajectory is approximately given by

$$\alpha_p(t) = 1 + 0.4\ t,$$

then a linear extrapolation would place the particle at a mass of 1730 Mev. No such resonance has been seen so far. Therefore, doubt exists on the very nature of the Pomeron trajectory as compared to other trajectories.

In this thesis, we shall investigate the nature of the Pomeron singularity and also for the comparison study the nature of the Rho trajectory.

There are several ways whereby a branch point and a pole can be experimentally distinguished. One, suggested by Gribov, utilizes the fact that a pole has a good parity but a branch point is unlikely to have a good parity. And the other uses the well known fact that a simple pole must have factorizable residues, whereas for a branch

point the factorization does not hold. In the next section, we show that there is every reason to believe that branch points exist in the J-plane.

6. Cuts in the J-plane

We include this section to show also that cuts can have dominant influence at high energy in elementary particle physics. In non-relativistic potential theory, the only singularities occurring in the J-plane to the right of the line Re $\ell = -\frac{1}{2}$, are the Regge poles. But theoretical arguments exist[8] that for hadron reactions, once Regge poles are introduced, the cuts in the J-plane are inevitable. These authors showed that cuts would normally exist if two Regge-poles are exchanged. Specific models have also been suggested that show how significant a part cut can play at high energy. It is shown that if $\alpha_1(t)$ and $\alpha_2(t)$ be two Regge poles, then the cut going to the left from a position $\alpha_C(t)$ in the J-plane is given by

$$\alpha_C(t) = \alpha_1(0) + \alpha_2(0) - 1 + \frac{\alpha_1' \cdot \alpha_2'}{\alpha_1' + \alpha_2'} t \ .$$

The main thing is to evaluate the influence of a cut at high energy. It is shown that the dominating contribution from the cut is given by

$$\beta_C(t) \left(\frac{s}{s_0} \right)^{\alpha_C(t)} \left(\log \frac{s}{s_0} \right)^{-\upsilon} \qquad \upsilon > 0 \ .$$

One can give examples to show that cut can play an important part. For example, take the charge-exchange reaction $\pi^- p \to \pi^0 n$, the cut can be due to P and ρ, and if $\alpha_P(0) = 1$, then

$$\alpha_C(t) > \alpha_\rho(t) \qquad \text{for} \quad t < 0.$$

In other words, the contribution of the cut is expected to dominate over the ρ-exchange contribution for all values of t except possibly at t = 0.

CHAPTER II

Factorization Test for the Pomeron in Three Particle Final States

1. Factorization Test

The one particle exchange (OPE) model has one characteristic property that coupling constants occur twice (fig. 2).

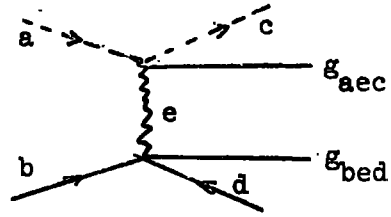

Figure 2

g_{aec} related to one vertex and g_{bed} to the other vertex. Now OPE model gives that its amplitude must be proportional to $g_{aec}\, g_{bed}$, that is, it factorizes into one contribution from each vertex. We see its parallel in one Regge-pole exchange.

For one pole contribution in Regge-pole model the amplitude α

$\beta(t)\ \xi(t) \left(\frac{s}{s_o} \right)^{\alpha(t)}$. If factorization holds, it turns out that the residue function

$$\beta(t) = (\text{known kinematical factors})\ \gamma_{a\bar{P}c}(t)\ \gamma_{\bar{b}Pd}(t)$$

in the t-channel.

There are two practical points of importance of this factorization property. Firstly it is the property of one Regge-pole exchange, and two Regge-poles or cut would desctroy factorization. Secondly one and the same Regge-pole coupling $\gamma_{a\bar{P}c}(t)$ may occur in different reactions, since it is independent of how the Regge-pole couples to the other two

particles. Therefore, it relates together different reactions. We explain this by an example: let pp, πp, $\pi\pi$ be elastic scatterings and assume asymptotic energy so that the Pomeron only contributes. Factorization implies $T^{el}_{pp} \alpha \gamma_{pPp}\, \gamma_{pPp}$; $T^{el}_{\pi p} \alpha \gamma_{\pi P\pi}\, \gamma_{pPp}$; $T^{el}_{\pi\pi} \alpha \gamma_{\pi P\pi}\, \gamma_{\pi P\pi}$. Hence factorization immediately yields the relation,

$$\sigma_{tot}(pp)\ \sigma_{tot}(\pi\pi) = (\sigma_{tot}(\pi p))^2 .$$

This is a safe theoretical prediction depending upon the exchange of one Regge-pole "P". So for $\sigma_{\pi\pi}$ e.s. total cross-section is not measurable experimentally at high energy, and so one is not able to test this hypothesis.

This conjecture of factorization can be studied in any diffraction dissociation process. Freund[9] applied this to the two body inelastic processes $pp \to pN^*$; $\pi p \to \pi N^*$ where N^* is a $T = 1/2$ nucleon resonance. In the latter case, the cross-sections are much smaller, but factorization could nevertheless be qualitatively tested and was found to hold with in errors. Since it was suggested[10] that Pomeron is not a pole, but a much more complicated singularity, it is therefore of great interest to study the factorization for all diffraction dissociation processes. To test the factorization for the Pomeron exchange, Freund applied the formula to elastic and inelastic reactions,

$$\frac{\frac{d\sigma}{dt}(pp\to pp)}{\frac{d\sigma}{dt}(\pi p\to \pi p)} \approx \frac{\frac{d\sigma}{dt}(pp\to pN^*(1400))}{\frac{d\sigma}{dt}(\pi p\to \pi N^*(1400))} \approx \frac{\frac{d\sigma}{dt}(pp\to pN^*(1688))}{\frac{d\sigma}{dt}(\pi p\to \pi N^*(1688))} .$$

At $t = 0$, the experimental data gives the values of the above equality 2.7, 3.2 and 2.9 respectively with background errors of 0.6. This means factorization holds for the Pomeron in this case. One can make

the conclusion that since the sum of a leading Pomeron and the Mandelstam cut it generates is not factorizable, the factorization of the Pomeron means that cut effects in such a model can be small.

Good and Walker's[11] idea that diffraction dissociation may play an important role in high energy hadron collisions has recently received strong support from a detailed analysis of 3, 4 and 5-body final states in pion-proton collisions. For the processes $\pi p \to 2\pi N$ (N = nucleon) and $\pi p \to 2\pi\Delta$ (1238 Mev) at 8 and 16 Gev/c are found to be [4,12] strongly dominated by the dissociations of the proton into πN and $\pi\Delta$ respectively. Similarly in four body reaction[13,14] $\pi^- p \to 2\pi^-\pi^+ p$ at 11 and 16 Gev/c and 5-body reaction $\pi^- p \to 2\pi^-\pi^+\pi^0 p$ has revealed marked diffraction dissociation. The lengthy technique for this evidence cannot be given here. But briefly it is based on the smallness and approximate constancy of transverse momenta and makes use of the appropriately weighted distributions in longitudinal phase space, thereby deriving from the bubble chamber data highly differential information on the collision amplitude.

2. Factorization for the Pomeron in Three Particle Final States

From the above experimental evidence it is useful to write the factorization formula and check it with the available experiments[15]. In this section we develop the theory to derive the test and then make conclusions by comparing it with the data at 10 Gev/c.

a) Derivation of the formula:-

First, take the reaction $\pi N \to \pi\pi N$ and let p and q be the initial four momenta of the nucleon and pion, respectively; k_1 and k_2 are the

final momenta of the pion and p' is the final nucleon momentum (fig. 3).

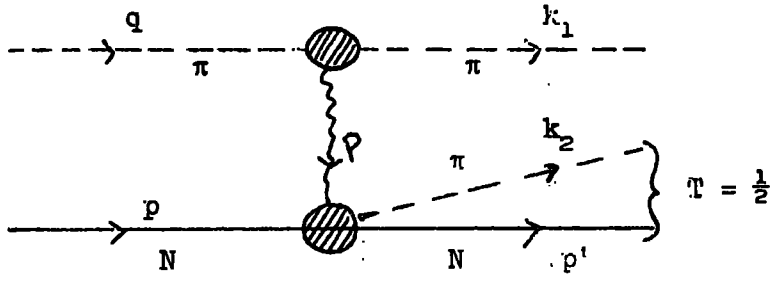

Figure 3

(Pomeron exchange in the reaction $\pi N \to \pi\pi N$)

The inelastic differential cross-section is given by

$$d\sigma_{in}(\pi) = \frac{1}{8(2\pi)^5} \frac{M^2}{\text{Flux}} F_{\pi\pi}(t)\, \xi(t)\, G(W^2, t)\delta^4(k_1 + k_2 + p' - q - p) \times \frac{d^3k_1}{w_1} \frac{d^3k_2}{w_2} \frac{d^3p'}{E'} \qquad (2.1)$$

where w_1, w_2 and E' are the energies of the final pions and the nucleon. M is the nucleon mass. The variables t and W^2 are given by

$$t = -(q - k_1)^2, \qquad W^2 = -(k_2 + p')^2$$

F and G are quantities

$$F_{\pi\pi}(t) = |< k_1, P|q >|^2$$

$$G(W^2, t) = \sum_{\text{spins}} |< k_2, p'|P,p >|^2$$

and $\sum_{\text{spins}}$ means sum over final spins and average over initial spins.

$\xi(t)$ represents the square of the exchanged trajectory's "propagator". Equation (2.1) simplifies to

$$d\sigma_{in}(\pi) = \frac{1}{8(2\pi)^5} \frac{M^2}{\text{Flux}} F_{\pi\pi}(t)\, \xi(t)\, G(W^2, t) \cdot \frac{d^3k_1}{w_1} \cdot \cdot \frac{\delta(w_1 + w_2 + E' - w - E)d^3p'}{w_2 E'} \cdot \tag{2.2}$$

Each of the last two factors in the equation (2.2) is Lorentz invariant and may be evaluated in any convenient frame. We evaluate it in the frame $\underline{k_2} + \underline{p'} = 0$, and label it by the subscript v. Now

$$W = (\underline{p_v'^2} + M^2)^{1/2} + (\underline{p_v'^2} + \mu^2)^{1/2}$$

where μ is the mass of the pion.

$$\therefore \quad \frac{dW}{dp_v'} = p_v'/E_v' + p_v'/w_{2v} = Wp_v'/(W_{2v} E_v') \tag{2.3}$$

Therefore

$$\frac{\delta(w_1 + w_2 + E' - w - E)d^3p'}{w_2 E'} = \frac{\delta(w_{1v} + W - w_v - E_v)d^3p_v'}{w_{2v} E'_v}$$

$$= \frac{\delta(w_{1v} + W - w_v - E_v)}{w_{2v} E_v'} p_v'^2 \frac{dp_v'}{d_v} d\Omega_{p_v'} = \left(\frac{p_v'}{W}\right) d\Omega_{p_v'} \cdot$$

Thus, we have

$$\frac{\delta(w_1 + w_2 + E' - w - E)d^3p'}{w_2 E'} = \left(\frac{p_v'}{W}\right) d\Omega_{p_v'} \tag{2.4}$$

Also

$$\frac{d^3k_1}{w_1} = \frac{d^3k_{1L}}{w_{1L}} = \frac{k_{1L}^2}{w_{1L}} \frac{dk_{1L}}{dw_{1L}} dw_{1L}\, d\Omega k_{1L} \tag{2.5}$$

where L denotes the laboratory frame $\underline{p} = 0$.

Now

$$w_{1L} = (k_{1L}^2 + \mu^2)^{1/2}$$

$$\therefore \quad (dw_{1L})/dk_{1L} = (k_{1L})/(w_{1L}) \tag{2.6}$$

From (2.5) and (2.6), we get

$$\frac{d^3k_1}{w_1} = k_{1L}\, dw_{1L}\, d\Omega_{k_{1L}}$$

$$= k_{1L}\, dw_{1L}(\sin\theta_{1L}\, d\theta_{1L})d\phi_{1L} \tag{2.7}$$

We now calculate the differential in (2.7) in terms of t and W^2. For that we need the relation

$$dt\, dW^2 = \begin{vmatrix} \frac{\partial t}{\partial(\cos\theta_{1L})} & \frac{\partial t}{\partial w_{1L}} \\ \frac{\partial W^2}{\partial(\cos\theta_{1L})} & \frac{\partial W^2}{\partial w_{1L}} \end{vmatrix} d(\cos\theta_{1L})dw_{1L} \tag{2.8}$$

Let us calculate the Jacobian.

$$t = -(q - k_1)^2 = 2\mu^2 + 2q.k_1$$

$$= 2\mu^2 + 2q_L k_{1L} \cos\theta_{1L} - 2w_L w_{1L} \tag{2.9}$$

with $k_{1L} = (w_{1L}^2 - \mu^2)^{\frac{1}{2}}$

$$W^2 = -(k_2 + p')^2 = -(q + p - k_1)^2$$

$$= s + \mu^2 + 2(q + p) \cdot k_1$$

$$= s + \mu^2 + 2(\underline{q} + \underline{p})_L \cdot k_{1L} - 2(q_o + p_o)_L w_{1L}$$

$$= s + \mu^2 + 2q_L k_{1L} \cos\theta_{1L} - 2(M + w_L)w_{1L} \cdot$$

(2.10)

From (2.9) and (2.10), we have

$$\frac{\partial t}{\partial(\cos\theta_{1L})} = 2q_L k_{1L} ; \qquad \frac{\partial t}{\partial w_{1L}} = 2q_L \frac{w_{1L}}{k_{1L}} \cos\theta_{1L} - 2w_L$$

$$\frac{\partial W^2}{\partial(\cos\theta_{1L})} = 2q_L k_{1L} ; \qquad \frac{\partial W^2}{\partial w_{1L}} = 2q_L \frac{w_{1L}}{k_{1L}} \cos\theta_{1L} - 2(M+w_L)$$

Hence, the Jacobian is

$$J = -4Mq_L k_{1L} .$$

Therefore, (2.8) reduces to

$$dt\, dW^2 = 4Mq_L k_{1L}(\sin\theta_{1L}\, d\theta_{1L})dw_{1L} \tag{2.11}$$

From (2.7), we have

$$\frac{d^3k_1}{w_1} = \frac{1}{4Mq_L} dt\, dW^2\, d\phi_{1L} . \tag{2.12}$$

Putting (2.4) and (2.12) in (2.2), and since Flux = Mq_L, we get

$$d\sigma_{in}(\pi) = \frac{1}{32(2\pi)^5} \cdot \frac{1}{q_L^2} \cdot F_{\pi\pi}(t) \cdot \xi(t) \cdot G(W^2, t)$$

$$\times (p_v'/W)\, d\Omega_{p_v'}\, dt\, dW^2\, d\phi_{1L} \tag{2.13}$$

The lower vertex in figure 3 represents the scattering

$$P + p \rightarrow k_2 + p' ,$$

where the mass-squared of the Pomeron is $-P^2 = -(q - k_1)^2 = t$.

The differential cross-section for this process is given by

$$d\sigma_p = \frac{M^2}{4(2\pi)^2} \cdot \frac{1}{\text{Flux}} \cdot \delta^4(k_2 + p' - P - p) G(W^2, t) \frac{d^3k_2}{w_2} \frac{d^3p'}{E'}$$

$$= \frac{M^2}{4(2\pi)^2} \cdot \frac{1}{\text{Flux}} \cdot G(W^2, t) \frac{\delta(w_2 + E' - P_o - E) d^3p'}{w_2 E'} \quad .$$

However, as before

$$\frac{\delta(w_2 + E' - P_o - E) d^3p'}{w_2 E'} = \frac{\delta(w_{2v} - E'_v - P_{ov} - E_v) d^3p'_v}{w_{2v} E'_v}$$

$$= \left(\frac{p'_v}{W} \right) d\Omega_{p'_v}$$

Hence,

$$d\sigma_p = \frac{M^2}{4(2\pi)^2 N} G(W^2, t) \left(\frac{p'_v}{W} \right) d\Omega_{p'_v}$$

$$\text{or} \qquad \int G(W^2, t) \left(\frac{p'_v}{W} \right) d\Omega_{p'_v} = 4(2\pi)^2 \frac{N}{M^2} \sigma_p (W^2, t) \qquad (2.14)$$

where N denotes the flux for the process and will cancel out from our relations eventually.

From (2.14) and (2.13), we obtain

$$d\sigma_{in}(\pi) = \frac{1}{8(2\pi)^3} \frac{N}{M^2 (q_L^\pi)^2} F_{\pi\pi}(t) \, \xi(t) \, \sigma_p(W^2, t) dt \, dW^2 \, d\Phi_{1L} \quad .$$

Integrating the R.H.S. with respect to Φ, we explicitly get

$$\frac{\partial^2 \sigma_{in}(\pi)}{\partial t \, \partial W^2} = \frac{1}{8(2\pi)^2} \frac{N}{M^2 (q_L^\pi)^2} F_{\pi\pi}(t) \, \xi(t) \, \sigma_p(W^2, t) \qquad (2.15)$$

(2.15) is the final form of the inelastic differential cross-section for the process $\pi N \rightarrow \pi\pi N$.

Similarly, we treat the process $NN \rightarrow \pi NN$ (Figure 4)

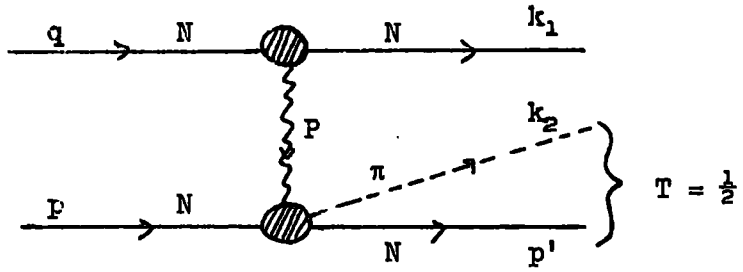

Figure 4

(Pomeron exchange in the reaction $NN \rightarrow N\pi N$).

The details of the calculation are the same as in the case of the first process. In this reaction we find,

$$\frac{\partial^2 \sigma_{in}(N)}{\partial t \, \partial W^2} = \frac{1}{2(2\pi)^2} \frac{N}{(q_L^N)^2} F_{NN}(t) \, \xi(t) \, \sigma_p(W^2, t) \qquad (2.16)$$

where $F_{NN}(t) = \sum_{\text{spins}} |< k_1, P|q >|^2$.

We now calculate the differential cross-section for the elastic scatterings $\pi N \rightarrow \pi N$ and $NN \rightarrow NN$ (Figure 5).

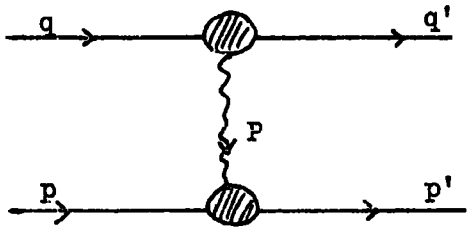

Figure 5

In the case of $NN \rightarrow NN$

$$d\sigma = \frac{M^4}{(2\pi)^2} \cdot \frac{1}{\text{Flux}} \cdot F_{NN}(t) \, \xi(t) \, F_{NN}(t) \frac{\delta(w' + p' - w - E) d^3 q'}{w^2 \, E'}$$

$$= \frac{M^4}{(2\pi)^2} \cdot \frac{1}{\text{Flux}} \cdot F_{NN}(t)\ \xi(t)\ F_{NN}(t)\ \frac{p}{W}\ d\Omega$$

$$= \frac{M^4}{2\pi} \cdot \frac{1}{\text{Flux}} \cdot F_{NN}(t)\ \xi(t)\ F_{NN}(t)\ \frac{p}{W}\ \sin\theta\ d\theta$$

Hence,

$$\frac{d\sigma_{e\ell}(N)}{dt} = \frac{1}{16\pi}\ \frac{M^4}{W^2 (p^N_{c.m.})^2}\ F_{NN}(t)\ \xi(t)\ F_{NN}(t) \qquad (2.17)$$

Similarly, for $\pi N \to \pi N$, we get

$$\frac{d\sigma_{e\ell}(\pi)}{dt} = \frac{1}{16\pi}\ \frac{M^2}{W^2 (p^\pi_{c.m.})^2}\ F_{\pi\pi}(t)\ \xi(t)\ F_{NN}(t) \qquad (2.18)$$

From (2.15) to (2.18), we get, at given values of W^2 and t,

$$\left(\frac{q^\pi_L}{q^N_L}\right)^2 \left[\frac{(\partial^2\sigma_{in}\ (\pi))/(\partial t\ \partial W^2)}{(\partial^2\sigma_{in}\ (N))/(\partial t\ \partial W^2)}\right] = \left(\frac{p^\pi_{c.m.}}{p^N_{c.m.}}\right)^2 \left[\frac{(d\sigma_{e\ell}(\pi))/dt}{(d\sigma_{e\ell}(N))/dt}\right] \qquad (2.19)$$

However, since

$$(q^\pi_L)^2 = \frac{1}{4M^2}\ [W^2 - (M+\mu)^2]\ [W^2 - (M-\mu)^2]$$

$$(q^N_L)^2 = \frac{W^2}{4M^2}\ (W^2 - 4M^2)$$

$$(p^\pi_{c.m.})^2 = \frac{1}{4W^2}\ [W^2 - (M+\mu)^2]\ [W^2 - (M-\mu)^2]$$

$$(p^N_{c.m.})^2 = \frac{1}{4}\ (W^2 - 4M^2)$$

From these expressions, we find that

$$\left(\frac{q^\pi_L}{q^N_L}\right)^2 = \left(\frac{p^\pi_{c.m.}}{p^N_{c.m.}}\right)^2 .$$

Hence, from (2.19), we obtain the factorization formula

$$\left[\frac{\partial^2\sigma_{in}(N)}{\partial t\,\partial W^2}\Big/\frac{\partial^2\sigma_{in}(\pi)}{\partial t\,\partial W^2}\right] = \left[\frac{d\sigma_{el}(N)}{dt}\Big/\frac{d\sigma_{el}(\pi)}{dt}\right] \qquad (2.20)$$

Equation (2.20) is the basic result of our calculations. The inelastic ratio on the left hand side for fixed t must remain approximately constant as W^2 is varied. This would by itself be an evidence for factorization.

b) Comparison with experiments

The above factorization test is expressed in terms of a double differential cross-section (at fixed momentum transfer and invariant mass of the two-particle subsystem in the final state) of the inelastic reactions. In applying it to the reactions $\pi N \to \pi\pi N$ and $NN \to \pi NN$, we find that experimental data at the same value of momentum transfer for the two reactions are not available. We have, therefore, averaged them over a range of momentum transfer $0.01 < |t| < 0.2$ $(Gev/c)^2$. It is obvious that Pomeron exchange in the two reactions discussed requires that the (πN) subsystem in the final state have $T = 1/2$. The $T = 1/2$ contributions in the data have been estimated by making use of the results of Boggild et al[16], who have shown that at the 19 (Gev/c) proton-proton interaction there is a predominance of 70% of the (πN) system in the isospin $T = 1/2$ state, and similarly in π^+p interactions, by the longitudinal phase-space considerations, there is a dominance of 80% of isospin-1/2 states of the (πN) system in the reactions,

$$\pi^+p \to \pi^+(\pi^+n) \quad \text{and} \quad \pi^+p \to \pi^+(\pi^0p) \quad \text{or} \quad \pi^+p \to \pi^0(\pi^+p)\ .$$

Experimentally[17] the curves of the inelastic πp and pp interactions relevant to our calculations are given as $\frac{\partial^2\sigma}{\partial t\,\partial p}$ mb/$(Gev/c)^3$

plotted versus the ratio p/p_{el} of particle momentum to that of elastically scattered particles at the same angle. For our purpose, we require to express the ratio p/p_{el} in terms of W.

For π^+p interaction, p/p_{el} can be expressed in W^2 as follows. (see Figure 6).

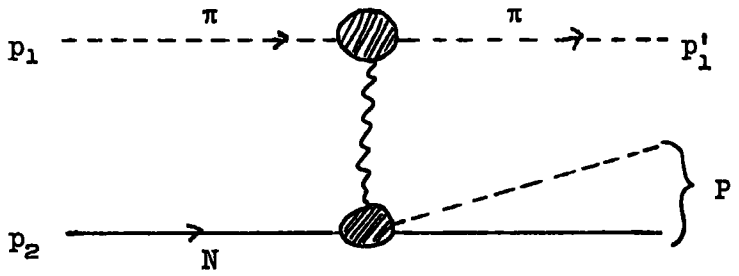

Figure 6

$$t_{inelastic} = -(p_2 - P)^2$$

$$= M^2 + W^2 + 2p_2 \cdot P \qquad (2.21)$$

Also energy-conservation gives

$$M + p_{1o}^L = p_{1o}'^L + P_o^L$$

In the laboratory frame, $\underline{p}_2 = 0$, therefore, from (2.21), we have

$$2M^2 + 2Mp_{1o}^L = 2Mp_{1o}'^L + 2MP_o^L$$

$$= 2Mp_{1o}'^L + M^2 + W^2 - t_{in}$$

i.e.

$$2M(p_{1o}'^L)_{in} = t_{in} + M^2 - W^2 + 2M\, p_{1o}^L \quad .$$

Also

$$2M(p_{1o}'^L)_{el} = t_{el} + 2M\, p_{1o}^L$$

or

$$\frac{p}{p_{e\ell}} = \frac{(p_1'^L)_{in}}{(p_1'^L)_{e\ell}} = \frac{t_{in} + M^2 - W^2 + 2M\, p_{1o}^L}{t_{e\ell} + 2M\, p_{1o}^L} \quad .$$

Now, since t is small, we can approximate the ratio by the formula

$$\frac{p}{p_{e\ell}} \approx \frac{M^2 - W^2 + 2M\, w_L}{2M\, w_L} \quad .$$

where w_L is the incident pion laboratory energy.

Similarly, for the pp interaction, we use the following formula to obtain the value of W from experimental given ratio $p/p_{e\ell} = x$ (say),

$$\frac{x(p_L)^2 + M^2}{(p_L)^2 + M^2} = \left(\frac{M^2 - W^2 + 2M\, E_L}{2M\, E_L} \right)^2$$

where E_L is the incident proton laboratory energy.

For the $\pi^+ p$ inelastic reaction, we use the date[17] at 10.02 Gev/c incident momenta in the range of momentum transfer $0.01 < |t| < 0.2$ $(\text{Gev/c})^2$, and for the pp interaction we use the data at 9.86 Gev/c incident momentum for the same range of momentum transfer. In Table I we give the experimental values of the ratio of the inelastic cross-sections for different values of the effective mass W of (πN) ranging from 1033 to 2113 Mev. In the ratio, we have taken into account only the $T = 1/2$ contribution at high energy, as explained in the beginning of this section. Similarly, Table II gives the ratios of the elastic differential cross-sections of pp and $\pi^+ p$ at 10.8 Gev/c incident momenta for values of momentum transfer in the range of $0.058 < |t| < 0.268$ $(\text{Gev/c})^2$.[18]

Table I Ratio of the Inelastic double differential cross-sections of pp and π^+p.

W(Mev)	Ratio	W(Mev)	Ratio	W(Mev)	Ratio	W(Mev)	Ratio
2133	2.28	1926	2.17	1719	2.34	1338	2.45
2091	2.31	1901	2.70	1691	2.42	1315	2.37
2068	2.31	1876	2.61	1663	2.58	1278	2.35
2045	2.35	1851	2.44	1634	2.50	1241	2.43
2022	2.44	1852	2.28	1483	2.17	1202	2.43
1998	2.50	1799	2.44	1451	2.32	1162	2.27
1974	2.61	1773	2.46	1418	2.40	1121	2.27
1950	2.71	1744	2.46	1384	2.33	1033	2.32

Table II Ratio of the elastic differential cross-sections of pp and π^+p.

- t	Ratio	- t	Ratio	- t	Ratio
0.058	2.48	0.157	2.16	0.256	2.31
0.084	2.39	0.203	2.29	0.268	2.10
0.116	2.33	0.250	2.20		

c) Results

The comparison of the two tables shows that the inelastic ratio varies from 2.71 to 2.17 and the elastic ratio varies from 2.48 to 2.10. Further, within the range of the variation $0.01 < |t| < 0.2$ $(Gev/c)^2$ in Table II, the ratio of the elastic differential cross-sections varies smoothly. This shows therefore, that our results agree with the factorization formula, thus favouring the possibility that the Pomeron singularity is a simple pole. Also we notice that the case discussed by Freund is a special case of our result. In addition, here we do not have any difficulty about the "background" which one has to subtract from the experimental results in order to find the resonances. We conclude by observing that since the usual Regge analysis of elastic processes involve more than the Pomeron, specially at 11 Gev/c, the comparison with inelastic scattering is surprisingly good.

CHAPTER III

Factorization Test for the Rho Trajectory

1. Introduction

As pointed out in Chapter I, it is an established fact now that in high energy scattering, other than simple Regge-poles in the J-plane, there can be dominant contributions due to the branch points. It is therefore of prime importance to study the nature of the dominating singularities.

Recent work[9,15,19] shows that there is a good evidence that the Pomeron singularity, which dominates diffraction scattering, is a simple pole. As one already knows and also from the analysis of recent experimental data on pp scattering[7] the Pomeron trajectory is different in many aspects from other dominating trajectories ρ, w, A_2, π and N, etc. Therefore any evidence for the Pomeron trajectory cannot be straight away taken to be true for other trajectories. On the other hand, the trajectories, ρ, w, A_2, π, N, ... etc. are similar, and once the nature of one such trajectory is established, then one must seriously look for similar behaviour for other trajectories.

In this chapter, we shall closely investigate the nature of the Rho-trajectory. Firstly, one must note that among other major trajectories, the Rho-trajectory is the only one that can participate in the charge-exchange reaction $\pi^- p \to \pi^0 n$, where it appears to be responsible for an α-dependent dip at $t = -0.6$, i.e. $\alpha_\rho(-0.6) = 0$[20]. The Rho-trajectory is also thought to be a leading participant in other charge-exchange reactions such as:

$$k^- p \to \bar{k}^0 n, \quad \pi n \to w\Delta, \quad \gamma p \to \rho n \ ;$$

$$\pi p \to \pi^0 \Delta^{++}, \quad \text{and} \quad \pi n \to wp \ .$$

Many fits to these reactions have been made, and the Rho-trajectory looks apparently linear in t and the values of the intercept vary between 0.52 and 0.65[21].

In the following sections we shall obtain a direct test for the Rho-factorization and then compare it with the available experimental data. We shall also see that in Rho-dominated reactions mixture of parities is being exchanged. Finally, we shall make some observations of our results about the nature of the Rho-trajectory.

2. Factorization Test for the Rho Trajectory

(a) Derivation of the formula

First, take the reaction $\pi N \to wN$, and let p,q be the initial four-momenta of the nucleon and pion respectively, q' and p' are the final momenta of w-particle and nucleon. The inelastic differential cross-section can be written as,

$$d\sigma_{in}^{(1)} = \frac{M^2}{4(2\pi)^2} \times \frac{1}{\text{Flux}} \times \frac{1}{w_2 E'} \times \delta^4 (q' + p' - q - p) \times$$

$$\times |< q', \rho | q >|^2 \, \xi(t) \sum_{\text{spins}} |< p' | \rho, \, p >|^2_{av} \times$$

$$\times \frac{d^3 q'}{(2\pi)^3} \cdot \frac{d^3 p'}{(2\pi)^3} \ . \qquad (3.1)$$

where w_2, E' are the energies the w-particle and final nucleon. Define

$$|< q', \rho|q >|^2 = F_{\pi w}(t)$$

$$\sum_{\text{spins}} |< p'|\rho, p >|^2_{av}$$

where $\sum_{\text{spins}}$ means sum over final spins and average over initial spins.

$\xi(t)$ represents the square of the Rho-trajectory exchange.

Further, the following quantities being Lorentz invariant are evaluated in the rest frame of the final nucleon state.

$$\frac{\delta^4(p' + q' - p - q)d^3p'd^3q'}{w_2E'} = \frac{\delta(w_2 + E' - w_1 - E)d^3q'}{w_2E'}$$

and

$$\frac{\delta(w_2 + E' - w_1 - E)d^3q'}{w_2E'} = \frac{p}{W} d\Omega$$

where w_1 and E are the initial energies of pion and nucleon. p is the initial (= final) centre of mass momenta and $W = -(p + q)^2$ is the total centre of mass energy. $d\Omega = \sin\theta\, d\theta\, d\phi$.

By definition, $t = -(q - q')^2$

$$= m_1^2 + m_2^2 + 2\underline{p}^2 \cos\theta - 2w_1w_2$$

m_1 and m_2 are masses of pion and w-particle.

$$dt = -2\underline{p}^2 \sin\theta\, d\theta \quad .$$

Putting all these values in (3.1) and integrating it with respect to ϕ , we finally get

$$\left(\frac{d\sigma}{dt}\right)_1 = \frac{M^2}{8(2\pi)} \times \frac{1}{\text{Flux}} \times \frac{1}{Wp} \times F_{\pi w}(t)\ \xi(t)\ F_{NN}(t). \qquad (3.2)$$

We need not know the value of the flux, because in the final results, the flux being the same, automatically cancels in all the reactions. Similarly take the second reaction $\pi N \rightarrow w\Delta^{++}$ and we obtain the final formula for the differential cross-section as

$$\left(\frac{d\sigma}{dt}\right)_2 = \frac{MM^*}{8(2\pi)} \times \frac{1}{\text{Flux}} \times \frac{1}{pW} \times F_{\pi w}(t)\ \xi(t)\ F_{\Delta n}(t) \qquad (3.3)$$

where

$$F_{\Delta N}(t) = \sum_{\text{spins}} |< p''|\rho,\ p >|^2_{av}$$

p'' and M^* are the four-momenta and mass of Δ^{++} respectively.

Similarly taking the third reaction of πN charge exchange, we get

$$\left(\frac{d\sigma}{dt}\right)_3 = \frac{M^2}{8(2\pi)} \times \frac{1}{\text{Flux}} \times \frac{1}{pW} \times F_{\pi\pi}(t)\ \xi(t)\ F_{NN}(t). \qquad (3.4)$$

The differential cross-section for the fourth reaction $\pi N \rightarrow \pi\Delta^{++}$ can be written as

$$\left(\frac{d\sigma}{dt}\right)_4 = \frac{MM^*}{8(2\pi)} \times \frac{1}{\text{Flux}} \times \frac{1}{pW} \times F_{\pi\pi}(t)\ \xi(t)\ F_{\Delta N}(t) \qquad (3.5)$$

Collecting all the results from (3.2) to (3.5) we finally get the factorization formula for the Rho-trajectory as

$$\frac{\frac{d\sigma(W)}{dt}(\pi^o p \rightarrow wp)}{\frac{d\sigma(W)}{dt}(\pi^+ p \rightarrow w^o \Delta^{++})} = \frac{\frac{d\sigma(W)}{dt}(\pi^- p \rightarrow \pi^o n)}{\frac{d\sigma(W)}{dt}(\pi^+ p \rightarrow \pi^o \Delta^{++})} \qquad (3.6)$$

The formula (3.6) is a basic result of our calculations. This must be tested at the same centre of mass energy W and at the same value of the momentum transfer t.

(b) Comparison with Experiments

Experimental data at nearly 4-5 Gev/c laboratory momenta exists for all the four inelastic reactions of equation (3.6). The cross-section data $d\sigma/dt$ versus $-t$ for $\pi^+ n \rightarrow p\omega^o$ have been taken at 5.1 Gev/c from Orsay-Bari-Bologna-Florence group [22].

Data for $\pi^+ p \rightarrow \omega^o \Delta^{++}$ at 5 Gev/c has been given by Bonn-Durham-Nijmegen-Paris-Strasbourg-Turin group[22].

Data for $\pi^- p \rightarrow \pi^o n$ [23] is at 4 Gev/c, and data for $\pi^+ p \rightarrow \pi^o \Delta^{++}$ at 4 Gev/c (see reference (22), page 105) have been used.

Table III gives the comparison of the two ratios in equation (3.6) versus negative value of the square of the momentum transfer. The data for all the four reactions is available upto $t = -0.55$ and beyond this reliable data does not exist.

(c) Result

Table III shows large statistical errors and therefore it excludes the exact interpretation of the data. Nevertheless, the comparison rules out simple factorization picture and apparently shows a significant failure of the factorization for the Rho-trajectory. On the other hand, there are two important points which have to be taken into consideration. Firstly, we have used the data at much lower energies, and therefore one cannot neglect the effect of lower trajectories, like B mesons, which contributes to omega production and is probably significant at lower energies. Secondly, cuts on the other hand should not spoil the factorization to any great extent. Therefore, we suggest that the breakdown of the factorization must be confirmed by good experiments at higher energies.

Table III

$-t$	$\frac{d\sigma}{dt}(\pi^+ n \to p w^o) / \frac{d\sigma}{dt}(\pi^+ p \to w^o \Delta^{++})$	$\frac{d\sigma}{dt}(\pi^- p \to \pi^o n) / \frac{d\sigma}{dt}(\pi^+ p \to \pi^o \Delta^{++})$
.05	.229 ± .033	.492 ± .049
.10	.200 ± .020	.542 ± .060
.15	.267 ± .055	.633 ± .180
.20	.212 ± .037	.473 ± .126
.25	.267 ± .044	.473 ± .094
.30	.300 ± .105	.591 ± .363
.35	.175 ± .07	.329 ± .09
.40	.480 ± .153	1.107 ± .553
.45	.480 ± .199	.738 ± .411
.50	.300 ± .100	.861 ± .557
.55	.360 ± .072	.953 ± .632
.60	.0 ± .02	---
.65	.20 ± .053	.329 ± .11
.70	.30 ± .09	---
.75	0 ± 0	---
.80	.40 ± .230	---

We also point out that our conclusion is not very surprising, since other evidence for the failure of factorization exists. A good example is $p\bar{p}$ and pp scattering, where it is necessary for a simple pole exchange, to have a zero in the w-residue at $t = -0.1$ $(Gev)^2$. This does not occur in the w-contribution to $\pi^+ n \rightarrow pn$, as it would have to do it factorization holds. Secondly, A_2 mesons are now experimentally identified to be two closely spaced resonances of identical quantum numbers, and therefore factorization of A_2 trajectory does not hold.

3. Exchange of Parity

Take the reactions $\pi N \rightarrow wN$ and $\pi N \rightarrow w\Delta^{++}$. The simplest production mechanism in these two reactions is the exchange of the Rho Regge-pole in the t-channel. We are interested in the decay correlation of the unstable particle w. Simple Rho exchange implies that $\rho_{00} = 0$, where $\rho_{mm'}$ is the density matrix element for the w expressed with respect to t-channel axis. Experimentally, ρ_{00} is 1/2 in the forward direction, indicating an appreciable amount of unnatural parity exchange. In many other reactions, the data is explained by adding another pole, but in this case even by adding B meson the calculated density matrix elements still do not agree.

We observe the following:

If natural parity $(-1)^J$ is exchanged in the above reactions, then

$$\rho_{00} = 0, \quad \text{Re } \rho_{10} = 0 \quad \text{and} \quad |\rho_{1-1}| \neq 0 .$$

If unnatural parity $(-1)^{J+1}$ is exchanged, then

$$\rho_{00} = 2N|F_{\nu_2 \nu_2', 00}(s,t)|^2, \quad \text{Re } \rho_{10} = 0, \quad |\rho_{1-1}| = 0 .$$

But experimentally[24], one finds ,

$$\rho_{00} \neq 0, \quad \text{and} \quad |\rho_{1-1}| \neq 0 .$$

The first indicates an appreciable amount of unnatural parity exchange, while the second, the natural parity exchange. This gives an indication that experimental data can be explained if mixture of parities is exchanged in the Rho-dominated reactions. This destroys the simple Rho-pole picture, and indicates that Regge-cuts may play an important part.

4. Conclusion

Failure of the factorization and mixture of parities exchanged can suggest that Rho-particle can be a parity doublet. This would not be very surprising since experimental evidence of A_2 parity doublet exists, and therefore, through exchange degeneracy one can suggest that if A_2 is a parity doublet, then so is Rho. One can also generalize these results and suggest that similar behaviour can exist for other low-lying meson trajectories.

CHAPTER IV

Parity Test for the Pomeron in Resonance Production Processes

1. Parity Test

In this chapter, we investigate another test for the Pomeron singularity suggested by Gribov[25]. Gribov, by the reggion graphic technique in the relativistic scattering problem, studied with respect to parity the effect of the Mandelstam cuts which are expected to be present. In the t-channel reaction a + b → c + d, Gribov shows that $P_r = (-1)^J P = +1$ for the Pomeron pole and $P_r = \pm 1$ for the Pomeron cut; where J is the total angular momentum and P the parity of a+ b state. This has important observational consequences. If we take c = d = proton and a and b are 0^- and 0^+ meson respectively, then $P_r = (-1)^J P = (-1)^J \eta_1 \eta_2 (-1)^L = -1$ since J = L for two mesons, η_1 and η_2 are opposite parities of the mesons. This means the Pomeron pole does not contribute; the Pomeron cut does. Another example, is the reaction $0^- + p \rightarrow 1^- + p$. The amplitude for the Pomeron pole exchange vanishes as sin θ in the forward direction, while the Pomeron-cut amplitude is small (in $\sqrt{-t}$) without vanishing. Gribov has not discussed such cases but one can mention that the same distinction could be applied when a is a proton and b is a proton isobar, the importance of the Pomeron-pole and the Pomeron contributions being essentially reversed, depending on the parity of the isobar.

We have used the above idea in the production of a single baryon or meson resonance in many two body reactions. Since in the regge-pole

model the nature of the exchange of states in the t-channel has a definite dependence on the polarization states of the resonances, therefore we have considered here the specific information contained in the final state polarization due to the exchange of definite parity for the Pomeron-pole and mixed parity for the Pomeron-cut.

Morrison[26] recently considered the contribution of the Pomeron to inelastic reactions such as $pp \to pN^*$ and $\pi^{\pm}p \to \pi^{\pm}N^*$. He noted that while other inelastic cross-sections decreased with energy, there is one constant energy case: that in which an N^* is produced from an initial nucleus for which the change in isospin is zero and the change in parity (ΔP) and the change in spin (ΔJ) obey $\Delta P = (-1)^{\Delta J}$. Similarly for meson resonance production Morrison found that for reactions where the change in quantum numbers between the resonance and the initial meson obey $\Delta T = 0$ and $\Delta P = (-1)^{\Delta J}$, the cross sections are nearly constant. We have, therefore, considered the processes $NN \to NN^*$ (N^*; $T = 1/2$, $J^P = 1/2^+$, $J^P = 3/2^-$) $\pi N \to \pi N^*$ (N^*; $T = 1/2$, $J^P = 1/2^+$, $J^P = (5/2^-)^+$) $\pi p \to Ap$ (A; $T = 1$, $J^P = 1^+$), $Kp \to K^*(1320)\, p$ (K^*, $T = 1$, $J^P = 1^+$) and $Kp \to K^*(1790)p$, (K^*, $T = 1/2$, $J^P = 2^-$) which are of diffractive nature. We use the fact that the Pomeron-pole and the Pomeron-cut have the same quantum numbers: signature P_j positive, isotopic spin zero, and positive G-parity. For the Pomeron-pole, in addition, definite parity is exchanged, therefore, with the available experimental data on differential-cross-sections we have computed the spin-space density matrix elements of different resonances for the pole exchange. In the presence of the Pomeron-cut, since mixture of parities with unknown ratio between them is exchanged, we predict results on the density matrix elements and also establish relations that are to be satisfied for the Pomeron-cut.

In the following section, we develop the Regge-pole formalism required for the single Pomeron dominant exchange and also state the conservation laws that have been used. In this case, we then compute, with the help of the experimental data, the relative magnitudes of the residue functions for different helicities of the Pomeron exchange. The knowledge of the residue functions then enables us to determine the density matrix elements of different resonances in different range of momentum transfer. We also make predictions for the Pomeron-pole and the Pomeron-cut separately. In conclusion, we shall suggest that experiments on the decay of unstable particles, studied in over reactions, be done to check the consistency of our results.

We have used helicity representation throughout and also used the following assumptions:

1) The same phases for the amplitudes belonging to different helcity states for the cut have been used.

2) The results are generally true to the leading order in the first power of the centre of the mass energy. At present laboratory energy, there can be sizeable corrections.

3) The residues are real functions of t and Pomeranchuk-Okun theorem holds, i.e. only the Pomeron contributes at high energy.

4) The helicity amplitudes for resonance production can be written as single dispersion relations in either energy or momentum transfer.

2. Regge-pole formalism

Consider the t-channel reaction $1 + 2 \rightarrow 3 + 4$. The partial wave expansion can be expressed in the helicity representation[27],

$$F_{\lambda_1\lambda_2,\lambda_3\lambda_4}(t,x) = (-1)^{\lambda-\lambda'}\sum_{J=\lambda}^{\infty}(J+\tfrac{1}{2})<\lambda_1\lambda_2|T^J(t)|\lambda_3\lambda_4>d^J_{\lambda\lambda'}(x) \tag{4.1}$$

where, $\lambda = \lambda_1 - \lambda_2$; $\lambda' = \lambda_3 - \lambda_4$, t is the square of the centre of mass energy in the t-channel and $x = \cos(\theta_t)$, θ_t being the scattering angle between particles 1 and 2. $d^J_{\lambda\lambda'}(x)$ is the usual rotation function and we follow the phase convention of Gunson and Andrews[28]. Changing the summation over J into the contour integration, and performing the usual Sommerfeld-Watson transformation[29], we can isolate the leading Regge-pole contribution to the helicity amplitudes ignoring other singularities as,

$$F_{\lambda_1\lambda_2,\lambda_3\lambda_4}(t,x) = -(-1)^{\lambda-\lambda'}\sum_{\substack{\mathrm{Re}\alpha>-\frac{1}{2}\\ \text{Regge poles}}}(\alpha+\tfrac{1}{2})\beta^{\pm}_{\lambda_1\lambda_2,\lambda_3\lambda_4}(t)$$

$$\times\, d^{\pm}_{\lambda,-\lambda'}(-x,\alpha)\times\frac{1}{\sin\pi(\alpha-\lambda)} \tag{4.2}$$

where $\beta^{\pm}$ are residues, the sign being positive or negative according as $J-\lambda$ is even or odd. The asymptotic behaviour of $d^{\alpha}_{\lambda\lambda'}(x)$ as $x\to\infty$, neglecting $1/x$ and higher powers (see equation (A.2) of ref. 29)

$$d^{\alpha}_{\lambda\lambda'}(x) = i^{\lambda-\lambda'}(\tfrac{1}{2}x)^{\alpha}\frac{\Gamma(2\alpha+1)}{[\Gamma(\alpha+\lambda+1)\Gamma(\alpha-\lambda+1)\Gamma(\alpha+\lambda'+1)\Gamma(\alpha-\lambda'+1)]^{\frac{1}{2}}} \tag{4.3}$$

and

$$d^{\pm}_{\lambda,-\lambda'}(-x,\alpha) = \tfrac{1}{2}\left[d^{\alpha}_{\lambda,-\lambda'}(-x) \pm d^{\alpha}_{\lambda,\lambda'}(x) \right]$$

since

$$d^{\alpha}_{\lambda,\lambda'}(x) = (-1)^{\alpha-\lambda}\, d^{\alpha}_{\lambda,-\lambda'}(-x)$$

We write the asymptotic behaviour for $d^{\pm}_{\lambda,-\lambda'}(-x,\alpha)$ as

$$d^{\pm}_{\lambda,-\lambda'}(-x,\alpha) = \tfrac{1}{2}\frac{(i)^{\lambda+\lambda'}\ (-\tfrac{1}{2}x)^{\alpha(t)}\ \Gamma(2\alpha+1)(1 \pm e^{-i\pi(\alpha-\lambda)})}{[\Gamma(\alpha+\lambda+1)\Gamma(\alpha-\lambda+1)\Gamma(\alpha+\lambda'+1)\Gamma(\alpha-\lambda'+1)]^{\frac{1}{2}}} .$$

Equation (4.2) can therefore be written as,

$$F_{\lambda_1\lambda_2,\lambda_3\lambda_4}(t,x) = -\pi(-1)^{\lambda-\lambda'} \sum_{\substack{\text{Re } \alpha > -\frac{1}{2} \\ \text{Regge poles}}} (\alpha(t)+\tfrac{1}{2}) \times \Gamma(2\alpha+1)$$

$$\times \left[\frac{1 \pm e^{-i\pi(\alpha-\lambda)}}{2 \sin \pi(\alpha-\lambda)} \right] \times \beta^{\pm}_{\lambda_1\lambda_2,\lambda_3\lambda_4}(t) \times (-\tfrac{1}{2}x)^{\alpha(t)}\ C_{\lambda\lambda'}(\alpha) \qquad (4.4)$$

where λ, λ' dependence has been explicitly taken out in

$$C^{(\alpha)}_{\lambda\lambda'} = \frac{i^{\lambda+\lambda'}}{[\Gamma(\alpha+\lambda+1)\Gamma(\alpha-\lambda+1)\Gamma(\alpha+\lambda'+1)\Gamma(\alpha-\lambda'+1)]^{\frac{1}{2}}} \qquad (4.5)$$

Further, since we consider Boson exchange,

$$\frac{1 \pm e^{-i\pi(\alpha-\lambda)}}{2 \sin \pi(\alpha-\lambda)} = \frac{(-1)^{\lambda} \pm e^{-i\pi\alpha}}{2 \sin \pi\alpha}$$

and this factor can be combined with $\beta^{\pm}(t)$ for all helicities.

Redefining

$$\beta^{\pm}_{\lambda_1\lambda_2,\lambda_3\lambda_4} = \beta^{\pm}_{\lambda_1\lambda_2,\lambda_3\lambda_4} \qquad \text{for even } \lambda$$

and

$$\beta^{\pm}_{\lambda_1\lambda_2,\lambda_3\lambda_4} = -\beta^{\pm}_{\lambda_1\lambda_2,\lambda_3\lambda_4} \qquad \text{for odd } \lambda \ .$$

Now $\pm$ sign corresponds to the signature of J in

$$\beta^{\pm}_{\lambda_1\lambda_2,\lambda_3\lambda_4}\left[\frac{1 \pm e^{-i\pi\alpha}}{2 \sin \pi\alpha}\right] \ .$$

Secondly, we absorb the t-dependence of $(-x/2)^{\alpha(t)}$ into the residue functions

$$\beta^{\pm}_{\lambda_1\lambda_2,\lambda_3\lambda_4}(t) = \left[\frac{-k_t q_t}{(M_1M_2M_3M_4)^{\frac{1}{2}}}\right]^{\alpha(t)} R^{\pm}_{\lambda_1\lambda_2,\lambda_3\lambda_4}$$

where

$$x\, k_t\, q_t = \frac{s - s_0(t)}{2}$$

and

$$s_0(t) = M_1^2 + M_2^2 - \frac{(t + M_1^2 - M_3^2)(t + M_2^2 - M_4^2)}{2t}$$

such that

$$\beta^{\pm}(t)(-\tfrac{1}{2}x)^{\alpha(t)} = \left[\frac{s - s_0(t)}{4(M_1M_2M_3M_4)^{\frac{1}{2}}}\right]^{\alpha(t)} R^{\pm}_{\lambda_1\lambda_2,\lambda_3\lambda_4}(t) \ .$$

Incorporating these results in equation (4.4), we finally obtain the formula for helicity amplitudes:

$$F_{\lambda_1\lambda_2,\lambda_3\lambda_4}(t,x) = -\pi(-1)^{\lambda-\lambda'} \sum_{\text{Regge poles}} (\alpha(t)+\tfrac{1}{2})\Gamma(2\alpha(t)+1)$$

$$\times\left[\frac{1 \pm e^{-i\pi\alpha}}{2\sin\pi\alpha}\right]\left(\frac{s - s_0(t)}{4(M_1M_2M_3M_4)^{\frac{1}{2}}}\right)^{\alpha(t)} R^{\pm}_{\lambda_1\lambda_2,\lambda_3\lambda_4}(t)\, C^{(\alpha)}_{\lambda\lambda'} \tag{4.6}$$

Differential cross-section in the s-channel can now be written and by crossing relation for helicity amplitudes[30], and including the normalization factor, the differential cross-section in terms of the t-channel amplitudes can be written as:

$$\frac{d\sigma}{dt} = \frac{\prod_i (2M_i)}{16\pi\left[(s - M_1^2 - M_2^2) - 4M_1^2M_2^2\right]} \times \frac{1}{(2s_1+1)(2s_2+1)}$$

$$\times \sum_{\lambda^s} |F_{\lambda_1\lambda_2,\,\lambda_3\lambda_4}(t,x)|^2$$

where the product of masses appears for the fermions only, and s_1 and s_2 are the spins of the initial particles. In this formalism, if one Regge-pole dominates, then the differential cross-section can be written as:

$$\frac{d\sigma}{dt} = \frac{\pi\prod_i (2M_i)}{64\left[(s - M_1^2 - M_2^2)^2 - 4M_1^2M_2^2\right]} \times \frac{1}{(2s_1+1)(2s_2+1)} \times (\alpha(t)+\tfrac{1}{2})^2$$

$$\times \left[\Gamma(2\alpha(t)+1)\right]^2 \times \left(\begin{matrix} 1 + \cot^2\frac{\pi\alpha(t)}{2} \\ + \tan^2\frac{\pi\alpha(t)}{2}\end{matrix}\right) \times \left(\frac{s - s_0(t)}{4(M_1M_2M_3M_4)^{\frac{1}{2}}}\right)^{2\alpha(t)}$$

$$\times \sum_{\lambda^s} \left|(-1)^{\lambda-\lambda'} R^{\pm}_{\lambda_1\lambda_2,\lambda_3\lambda_4}(t)\, C^{(\alpha)}_{\lambda\lambda'}\right|^2 . \tag{4.7}$$

The above form is for $s \to \infty$, or $x \to -\infty$, with t finite and negative. This is the main formula, which we shall use to find the unknown residue functions.

3. Conversation Laws

(i) The parity conservation law: This law holds among strongly interacting particles and it reduces the number of amplitudes to half. Following Jacob and Wick[27], we have

$$F_{-\lambda_1-\lambda_2,-\lambda_3-\lambda_4} = \frac{\eta_3\,\eta_4}{\eta_1\,\eta_2}(-1)^{(s_3+s_4)-(s_1+s_2)}(-1)^{\lambda-\lambda'}F_{\lambda_1\lambda_2,\lambda_3\lambda_4} \tag{4.8}$$

where η_i is the intrinsic parity of the particle i.

(ii) The G-parity conservation law: In the cases where the two particles in the initial state of t-channel are $N\bar{N}$, this implies restrictions on the amplitudes. The use of the asymptotic property of the d-functions (equation (4.3)), and the definition of the G-parity at $N\bar{N}$ state,

$$G|J,\ \lambda_N\ \lambda_{\bar{N}}> \ =\ (-1)^{J+T}\ |J,\ \lambda_{\bar{N}}\ \lambda_N> \ .$$

We derive this relation involving G-parity by writing the amplitude as

$$F_{\lambda_3\lambda_4,\lambda_N\lambda_{\bar{N}}} = M\sum_J (2J+1) < \lambda_3\lambda_4|T^J(t)|\lambda_N\lambda_{\bar{N}} > d^J_{\lambda_N-\lambda_{\bar{N}},\lambda_3-\lambda_4}$$

$$= M\sum_J (2J+1) < \lambda_3\lambda_4|T_1^J(t)\ G|\lambda_g > < \lambda_g|T_2^J(t)G|\lambda_N\lambda_{\bar{N}} > d^J_{\lambda\mu}(\theta)$$

$$= Mg(-1)^J(-1)^T(-1)^{\lambda_N-\lambda_{\bar{N}}}\sum_J (2J+1) < \lambda_3\lambda_4|T^J(t)|\lambda_{\bar{N}}\lambda_N > d^J_{-\lambda\mu}(\theta).$$

Hence the relation

$$F_{\lambda_3\lambda_4,\lambda_N\lambda_{\bar{N}}} = (-1)^{\lambda} g\, P_j (-1)^T F_{\lambda_3\lambda_4,\lambda_{\bar{N}}\lambda_N} \qquad (4.9)$$

where g is the G-parity of the Pomeron. In our analysis we shall take $g\, P_j(-1)^T$ = +ve, for all the reactions. In this case, the Pomeron pole, cut, and also P', ρ, w, φ, π, etc. Regge-poles and the branch points arising from the exchange of these poles and n-vacuum poles can be exchanged. Through our assumption (3) we exclude all poles like: π, ρ, ... of the isotopic spin one at high energy. Table IV for $gP_j(-1)^T$ = positive, gives the possible trajectories that can be exchanged.

T	g	P_j	Associated trajectories
0	+	+	P,P',A,B,C,f,χ,η, ...
0	-	-	w,φ, ...
1	+	-	ρ, ...
1	-	+	π, A_2, ...

Table IV

Trajectories exchanged due to $gP_j(-1)^T$ = positive

(iii) The law of definite parity exchange: We use the definite parity conserving amplitudes. By taking linear combinations of helicity states, we construct states of definite parity and form parity conserving partial waves amplitudes of $(-1)^J$ and $(-1)^{J+1}$ parities, as partial waves amplitudes can have contributions from states of both, even and odd parity. Keeping track of the number of such combinations of partial waves amplitudes, we deduce by the method given below the relation for $(-1)^J$ and $(-1)^{J+1}$.

$$F_{\lambda_1\lambda_2,\lambda_3\lambda_4}(t,x) = (-1)^{\lambda-\lambda'} \sum_J (2J+1) < \lambda_1\lambda_2|T^J(t)|\lambda_3\lambda_4 > d^J_{\lambda\lambda'}(x)$$

$$= (-1)^{\lambda-\lambda'} \sum_J (2J+1) < \lambda_1\lambda_2|P|\lambda_p >< \lambda_p|PT^J(t)|\lambda_3\lambda_4 > \times d^J_{\lambda\lambda}(x)$$

If $P|\lambda_p > = (-1)^J|\lambda_p >$

$P|\lambda_1\lambda_2 > = (-1)^{J+s_1+s_2}\ \eta_1\eta_2|-\lambda_1-\lambda_2 >$

then

$$F_{\lambda_1\lambda_2,\lambda_3\lambda_4}(t,x) = \eta_1\eta_2(-1)^{\lambda}\ (-1)^{s_1+s_2}\ F_{-\lambda_1-\lambda_2,\lambda_3\lambda_4}$$

Therefore,

(I) If $(-1)^J$ parity is exchanged in the intermediate state, then

$$F_{\lambda_1\lambda_2,\lambda_3\lambda_4}(t,x) = \eta_1\eta_2(-1)^{s_1+s_2}\ (-1)^{\lambda}\ F_{-\lambda_1-\lambda_2,\lambda_3\lambda_4}$$

Similar relation holds for the other vertex.

(II) If $(-1)^{J+1}$ parity is exchanged in the intermediate state, then

$$F_{\lambda_1\lambda_2,\lambda_3\lambda_4} = -\eta_1\eta_2(-1)^{s_1+s_2}\ (-1)^{\lambda}\ F_{-\lambda_1-\lambda_2,\lambda_3\lambda_4}$$

These two relations enable us to put restrictions on the amplitudes in case of the Pomeron-pole and cut[31].

4. Expressions for the density matrix elements

The most convenient form of the expression for the density matrix elements expressed by continuing in terms of the t-channel helicity amplitudes is given by Gottfried and Jackson[32],

$$\rho_{mm'} = N \sum_{\lambda_1\lambda_2\lambda_3\lambda_4} F_{\lambda_1\lambda_2,\lambda_3 m} F^*_{\lambda_1\lambda_2,\lambda_3 m'}$$

where the normalization constant N is fixed by the condition that the trace of matrix $\rho_{mm'} = 1$, and m, m' are the helicity quantum numbers of the resonance. For convenience, we shall while writing, denote m, m' as twice the actual values of the helicity numbers.

The number of independent measurable density matrix elements for half integer spin J are:

$$\begin{aligned} &\rho_{mm} && 1 < m \leq 2J \\ &\text{Re } \rho_{mn} && n < m \leq 2J \\ &\rho_{m-m} && 0 < m \leq 2J \end{aligned}$$

and in case of integer spin J,[33]

$$\begin{aligned} &\rho_{mm} && 0 < m \leq J \\ &\text{Re } \rho_{mn} && |n| < m \leq J \\ &\rho_{m-m} && 0 < m \leq J \ . \end{aligned}$$

Using equation (4.6), we express the density matrix for our purpose as,

$$\rho_{mm'} = \frac{\sum^s R^{\pm}_{\lambda_1\lambda_2,\lambda_3 m} R^{\pm}_{\lambda_1\lambda_2,\lambda_3 m'} C_{\lambda_1-\lambda_2,\lambda_3-m}(\alpha) C^*_{\lambda_1-\lambda_2,\lambda_3-m'}(\alpha)}{N_p(t)} \qquad (4.10)$$

where,

$$N_P(t) = |(-1)^{\lambda-\lambda'} R^{\pm}_{\lambda_1\lambda_2,\lambda_3\lambda_4}(t)\, C_{\lambda\lambda'}(\alpha)|^2$$

$N_P(t)$ is calculated from the formula (4.7) by fitting the available data on differential cross-sections for different processes. This enables us then, to find the residue functions for different helicity states of the Pomeron exchange. Since $C_{\lambda\lambda'}(\alpha)$ are known, we can compute $\rho_{mm'}(t)$ for the given range of momentum transfer.

5. Application to different processes and predictions

(A) $NN \to NN^*$.

(i) For $N^*(1400)$, $J^P = (1/2)^+$, $T = 1/2$ we are left with six helicity amplitudes after applying the conservation laws.

For Pomeron-pole $P_r = (-1)^J P = +1$, hence only $(-1)^J$ parity conserving amplitudes contribute. We are therefore left with the following four independent amplitudes:

$$F_{1/2\ 1/2;\ 1/2\ 1/2}\ ; \quad F_{1/2\ 1/2,\ 1/2\ -1/2}$$

$$F_{1/2\ -1/2;\ 1/2\ 1/2}\ ; \quad F_{1/2\ -1/2,\ 1/2\ -1/2}\ .$$

The differential cross-section for the Pomeron pole at high energy can be written from the above formula

$$\frac{d\sigma}{dt} = \frac{\pi M^3 M^*}{4[\ s(s-4M^2)\ ]} \times (\alpha_p(t)+1/2)^2 \times [\Gamma(2\alpha_p(t)+1)]^2 \times$$

$$\times \left(1+\cot^2\frac{\pi\alpha_p(t)}{2}\right) \times \left(\frac{s-\frac{1}{2}(3M^2+M^{*2}-t)}{4(M^3M^*)^{\frac{1}{2}}}\right)^{2\alpha_p(t)} \times N_p(t)$$

where

$$N_p(t) = R^2_{1/2\ 1/2,1/2\ 1/2}(t)|C_{oo}|^2 + (R^2_{1/2\ -1/2,1/2\ 1/2}(t) + R^2_{1/2\ 1/2,1/2\ -1/2}) \times |C_{10}|^2 + R^2_{1/2\ -1/2,1/2\ -1/2}|C_{11}|^2 \ .$$

There is only one independent density matrix element ρ_{1-1} for which the absolute value of ρ_{1-1} for N* is given by

$$|\rho_{1-1}(t)| = (R_{1/2\ 1/2,1/2\ 1/2}\, R_{1/2\ -1/2,1/2\ 1/2}|C_{oo}||C_{o1}| - R_{1/2\ 1/2,1/2\ -1/2}\, R_{1/2\ -1/2,1/2\ -1/2}|C_{o1}||C_{11}|) \Big/ (N_p(t))$$

Individual residues must be determined to calculate $|\rho_{1-1}(t)|$. We have used the data for $pp \rightarrow pN^*(1400)$ given by Anderson et al.[34] at the incident laboratory momenta of 10, 15, 20 and 30 Gev/c in the range of momentum transfer $-0.14 \leq t \leq -0.013$ $(Gev/c)^2$. Our input for the parameters of the Pomeron trajectory is $\alpha_p(t) = 1 + (0.4 \pm 0.07)t$, which has been taken for the latest high energy data of Serpukhov[7]. We have also assumed the residues to be linear functions of t, i.e. $R_i^2(t) = \alpha_i + \beta_i t$ where α_i and β_i are the constraints to be determined for each residue $R_i^2(t)$. The unknown function of t, $N_p(t)$ is determined by fitting the curve of the above data, the average value found for the range of momentum transfer $-0.14 \leq t \leq -0.013$ $(Gev/c)^2$ is

$$N_p(t) = 5.828 \pm 0.9 \text{ mb.}$$

The residue functions in this range of momentum transfer are,

$$10^{-6}\, R^2_{1/2\ 1/2,1/2\ 1/2} = -(0.084 \pm 0.01) - (0.353 \pm 0.04) \text{ mb}$$

$$10^{-6}\, R^2_{1/2\ -1/2,1/2\ 1/2} = 10^{-6}\, R^2_{-1/2\ -1/2,1/2\ -1/2} = (1.701 \pm .05) - (1.518 \pm .01)t \text{ mb}$$

$$10^{-6}\, R^2_{1/2\ -1/2,1/2\ -1/2} = (14.35 \pm .8) + (1.51 \pm .08)t \text{ mb.}$$

With these values of the residue functions, we obtain the graph No. I for $|\rho_{1-1}|$ against t. This increases uniformly from zero at t = 0 to the maximum value 1 at t = -0.13. It is suggested, that experiments on the decay of N*(1400) be done to compare with the curve obtained theoretically by us under the assumption of the single Pomeron pole exchange.

For the Pomeron-cut, $P_r = \pm 1$, therefore both $(-1)^J$ and $(-1)^{J+1}$ parity conserving amplitudes would contribute with an unknown ratio of parity between them. The following relations of helicity amplitudes would hold in the presence of the Pomeron-cut:

$$F_{1/2\ 1/2,1/2\ 1/2} = F_{-1/2\ -1/2,-1/2\ -1/2} = \pm F_{-1/2\ -1/2,1/2\ 1/2} = \pm F_{1/2\ 1/2,-1/2\ -1/2}$$

$$F_{1/2\ 1/2,1/2\ -1/2} = -F_{-1/2\ -1/2,-1/2\ 1/2} = \pm F_{-1/2\ -1/2,1/2\ -1/2} = \mp F_{1/2\ 1/2,-1/2\ 1/2}$$

$$F_{1/2\ -1/2,1/2\ 1/2} = -F_{-1/2\ 1/2,-1/2\ -1/2} = -F_{-1/2\ 1/2,1/2\ 1/2} = F_{1/2\ -1/2,-1/2\ -1/2}$$

$$F_{1/2\ -1/2,1/2\ -1/2} = F_{-1/2\ 1/2,-1/2\ 1/2} = -F_{-1/2\ 1/2,1/2\ -1/2} = -F_{1/2\ -1/2,-1/2\ 1/2}$$

Writing the expression for $|\rho_{1-1}|$ under the restrictions $P_r = \pm 1$, we find that its only difference from the pole is that at different values of t in the above range of momentum transfer the value of $|\rho_{1-1}|$ becomes approximately zero. Hence for the cut, the curve will not be smooth like that of the pole, but will have discontinuities in the function $|\rho_{1-1}(t)|$ at different values of t.

(ii) For N*(1520), $J^P = (3/2)^-$, $T = 1/2$.

For the Pomeron pole, applying all the conservation laws and for $P_r = +1$ exchange, we are left with only eight helicity amplitudes. The differential cross-section for the pole is,

$$\frac{d\sigma}{dt} = \frac{\pi M^3 M^*}{4[s(s-4M^2)]} \times (\alpha_p(t) + 1/2)^2 \times [\Gamma(2\alpha_p(t) + 1)]^2$$

$$\times \left(1 + \cot^2 \frac{\pi\alpha_p(t)}{2}\right) \times \left(\frac{s - 1/2(3M^2 + M^{*2} - t)}{4(M^3M^*)^{\frac{1}{2}}}\right)^{2\alpha_p(t)} \times N_p(t)$$

where

$$N_p(t) = R^2_{1/2\ 1/2,1/2\ 1/2}(t)|C_{oo}|^2 + (R^2_{1/2\ -1/2,1/2\ -1/2}(t)$$

$$+ R^2_{1/2\ -1/2,1/2\ 3/2}(t))|C_{11}|^2 + (R^2_{1/2\ -1/2,1/2\ 1/2}(t)$$

$$+ R^2_{1/2\ 1/2,1/2\ -1/2}(t) + R^2_{1/2\ 1/2,1/2\ 3/2}(t))|C_{10}|^2$$

$$+ R^2_{1/2\ 1/2,1/2\ -3/2}|C_{02}|^2 + R^2_{1/2\ -1/2,1/2\ -3/2}|C_{12}|^2 \ .$$

There are five independent density matrix elements in which ρ_{33}, $i\rho_{3-3}$ and $i\rho_{1-1}$ are real. ρ_{33}, $\mathrm{Re}(\rho_{31})$, $\mathrm{Re}(\rho_{3-1})$ enter in the decay distribution of N* and the parameters ρ_{3-3}, ρ_{1-1} contribute to other observables such as spin correlation, therefore these can be measured easily in the experiments. We have computed the values of ρ_{33}, $\mathrm{Re}(\rho_{31})$ and $\mathrm{Re}(\rho_{3-1})$ for the single Pomeron pole exchange. We have,

$$\rho_{33} = (1/2(R^2_{1/2\ 1/2,1/2\ 3/2}|C_{10}|^2 + R^2_{1/2\ -1/2,1/2\ 3/2}|C_{11}|^2$$

$$+ R^2_{1/2\ 1/2,1/2\ -3/2}|C_{02}|^2 + R^2_{1/2\ -1/2,1/2\ -3/2}|C_{12}|^2)) \Big/ N_p(t)$$

$$\text{Re } \rho_{31} = -1/2\Big[R_{1/2\ 1/2,1/2\ 1/2}\, R_{1/2\ 1/2,1/2\ 3/2}|C_{00}||C_{0-1}|$$

$$+ R_{1/2\ -1/2,1/2\ 1/2}\, R_{1/2\ -1/2,1/2\ 3/2}|C_{1-1}||C_{10}|$$

$$- R_{1/2\ 1/2,1/2\ -3/2}\, R_{1/2\ 1/2,1/2\ -1/2}|C_{01}||C_{02}|$$

$$- R_{1/2\ -1/2,1/2\ 1/2}\, R_{1/2\ -1/2,1/2\ -3/2}|C_{10}||C_{12}|\Big] \Big/ N_p(t)$$

$$\text{Re } \rho_{3-1} = 1/2\Big[R_{1/2\ 1/2,1/2\ -1/2}\, R_{1/2\ 1/2,1/2\ 3/2}\, C_{0-1}C^*_{01}$$

$$+ R_{1/2\ -1/2,1/2\ -1/2}\, R_{1/2\ -1/2,1/2\ 3/2}|C_{1-1}||C_{11}|$$

$$+ R_{1/2\ 1/2,1/2\ 1/2}\, R_{1/2\ 1/2,1/2\ -3/2}|C_{02}||C_{01}|$$

$$+ R_{1/2\ -1/2,1/2\ 1/2}\, R_{1/2\ -1/2,1/2\ -3/2}|C_{10}||C_{12}|\Big] \Big/ N_p(t)$$

where

$$N_p(t) = R^2_{1/2\ 1/2,1/2\ 1/2}(t)|C_{00}|^2 + (R^2_{1/2\ -1/2,1/2\ 1/2}(t)$$

$$+ R^2_{1/2\ 1/2,1/2\ -1/2}(t)\,)|C_{11}|^2 + (R^2_{1/2\ -1/2,1/2\ -1/2}(t)$$

$$+ R^2_{1/2\ 1/2,1/2\ 3/2}(t) + R^2_{1/2\ -1/2,1/2\ 3/2}(t)\,)|C_{10}|^2$$

$$+ R^2_{1/2\ 1/2,1/2\ -3/2}|C_{02}|^2 + R^2_{1/2\ -1/2,1/2\ -3/2}|C_{12}|^2 .$$

Data on the differential cross-section[34] is used for 10, 15, 20 and 30 Gev/c incident laboratory momenta in the range of momentum transfer $-0.833 \leq t \leq -0.252$. Our in-put is the same as in the case of N*(1400) for the parameters of the Pomeron trajectory. The unknown function of $N_p(t)$ is determined, its average value in the above range taken at 16 different values of t is 0.6023 ± 0.05 mb. Individual residue functions are also determined in order to calculate the values

of spin density matrix elements. The residue functions are for $-0.833 \leq t \leq -0.252$,

$$10^{-6} R^2_{1/2\ 1/2,1/2\ 1/2}(t) = (0.3012 \pm 0.1) + (0.1232 \pm 0.04)t \text{ mb.}$$

$$10^{-6} R^2_{1/2\ -1/2,1/2\ 1/2}(t) = 10^{-6} R^2_{1/2\ 1/2,1/2\ -1/2}(t)$$
$$= 10^{-6} R^2_{1/2\ 1/2,1/2\ 3/2}(t) = (1.032 \pm 0.04) - (0.258 \pm 0.01) \text{ mb}$$

$$10^{-6} R^2_{1/2\ -1/2,1/2\ -1/2}(t) = 10^{-6} R^2_{1/2\ -1/2,1/2\ -3/2}(t)$$
$$= (0.8595 \pm 0.2) - (1.232 + 0.02)t \text{ mb}$$

$$10^{-6} R^2_{1/2\ 1/2,1/2\ -3/2}(t) = (1.8002 \pm 0.09) + (1.3223 \pm 0.05)t \text{ mb}$$

$$10^{-6} R^2_{1/2\ -1/2,1/2\ -3/2}(t) = (7.763 \pm 0.4) - (2.166 + 0.1)t \text{ mb.}$$

With the help of these residue functions we plot three curves (Graph II) for the values of ρ_{33}, $\mathrm{Re}(\rho_{31})$ and $\mathrm{Re}(\rho_{3-1})$ against t. Experiments on the decay of N*(1520) are suggested to compare with the values obtained by us.

For the Pomeron-cut, we can only make a general observation, $P_r = -1$ contributes to only four amplitudes, all other amplitudes vanish due to the contradiction with the positive G-parity of the Pomeron exchange. We write the expressions for the density matrix elements, which gives for $P_r = -1$ values lying below the values obtained for $P_r = +1$. Hence, for the Pomeron-cut the points of ρ_{33}, $\mathrm{Re}(\rho_{31})$ and $\mathrm{Re}(\rho_{3-1})$ against t either lie on the curves of Graph II or below it, but cannot be above the curves. Further, the curve for the Pomeron-cut must have discontinuities, unlike the curves of the Pomeron-pole.

(B) $\pi N \rightarrow \pi N^*$

(i) N*(1400), $J^P = (1/2)^+$, $T = 1/2$.

In this reaction, in the t-channel, $P_r = +1$ always, therefore only

the Pomeron-pole contributes. It is of interest here to compute the values of $|\rho_{1-1}|$ for the Pomeron-pole to compare and check with the values obtained in the reaction $NN \rightarrow NN^*(1400)$. Applying the conservation laws, we are left with only two amplitudes. The differential cross-section is

$$\frac{d\sigma}{dt} = \frac{\pi M M^*}{16[s-\mu^2-M^2)^2 - 4\mu^2M^2]} \times (\alpha_p(t) + 1/2)^2 \times [\Gamma(2\alpha_p(t)+1)]^2$$

$$\times \left[1 + \cot^2 \frac{\pi\alpha_p(t)}{2}\right] \times \left[\frac{s - \frac{1}{2}(2\mu^2 + M^2 + M^* - t)}{4\mu(MM^*)^{\frac{1}{2}}}\right]^{2\alpha_p(t)} \times N_p(t)$$

where

$$N_p(t) = R^2_{oo,1/2\ 1/2}|C_{oo}|^2 + R^2_{oo,1/2\ -1/2}|C_{o1}|^2$$

and

$$|\rho_{1-1}| = \frac{R_{oo,1/2\ 1/2}(t)\, R_{oo,1/2\ -1/2}(t)|C_{o1}||C_{oo}|}{N_p(t)} .$$

Recent data on $\pi N \rightarrow \pi N^*$ at 8 Gev/c and 16 Gev/c laboratory momenta are given by Anderson et al[35]. Using this data, we obtain the values of the residue functions for $0.02 \leq -t \leq 0.13$ as

$$10^{-3}\, R^2_{oo,1/2\ 1/2}(t) = (0.8633 \pm 0.05) + (0.304 \pm 0.06)t \text{ mb}$$

$$10^{-3}\, R^2_{oo,1/2\ -1/2}(t) = (1.725 \pm 0.35) - (0.306 \pm 0.06)t \text{ mb}$$

The curve of $|\rho_{1-1}|$ obtained in this case (Graph III) is the same as in Graph I. It smoothly varies from 0.2 to 0.9 in the same range of momentum transfer, confirming that the single Pomeron-pole exchange cannot have discontinuities as found in the case of the branch point in the reaction $NN \rightarrow NN^*(1400)$.

(ii) $N^*(1690)$, $J^P = (5/2)^{\pm}$, $T = 1/2$.

Here again only the Pomeron-pole contributes, and we have used the data in the range $0.02 \leq -t \leq 0.22$ at 8 Gev/c and 16 Gev/c incident laboratory momenta[35]. Using the previous method, we obtain all the residues and compute the values of the independent measurable density matrix elements. The values of ρ_{55}, ρ_{33}, ρ_{53}, ρ_{51}, ρ_{5-1}, ρ_{5-3}, ρ_{31} and ρ_{3-1} are given in the Graphs IV, V and VI. ρ_{5-5} and ρ_{3-3} vanish identically. We suggest, that experiments on the decay distribution of $N^*(1690)$ be done to compare with the results obtained theoretically by us.

(C) $\pi^+ p \rightarrow A_1^+ p$; $Kp \rightarrow K^*(1320)p$.

Both the produced resonances have the same quantum numbers except the masses. K^* and A_1 have $J^P = 1^+$ and $T = 1$. In the t-channel, the Pomeron-pole and the Pomeron-cut can be exchanged.

For the Pomeron-pole only four amplitudes contribute,

$$F_{1/2\ 1/2,0\ 1};\quad F_{1/2\ -1/2,0\ 1};\quad F_{1/2\ 1/2,0\ 0};\quad F_{1/2\ -1/2,0\ 0}\ .$$

So we have the following relations between the density matrix elements,

$$\rho_{11} + \rho_{1-1} = 0 \quad \text{and} \quad 2\rho_{11} + \rho_{00} = 0\ .$$

Contribution of ρ_{00} is only due to the Pomeron-pole.

For the Pomeron-cut, we have, $\rho_{11} + \rho_{1-1} = 2N|F_{1/2\ 1/2,0\ 1}|^2$ where N is the inverse of the differential cross-section of the process at $t = 0$. There would not be any contribution from the cut to ρ_{00}. Data on the above process does not exist. These reactions are extremely favourable to give a definite prediction on the nature of the Pomeron,

and therefore, experiments on the decay of A_1^+ and K* are suggested.

(D) $Kp \rightarrow K^*(1790)p$.

$K^*(1790)$; $J^P = (2)^-$ and $T = 1/2$.

Applying the parity and G-parity conservation laws, we are left with eight helicity amplitudes.

For the Pomeron-pole the following six parity conserving amplitudes contribute:

$$F_{1/2\ 1/2,02}\ ;\quad F_{1/2\ -1/2,\ 02}\ ;\quad F_{1/2\ 1/2,01}$$

$$F_{1/2\ -1/2,01}\ ;\quad F_{1/2\ 1/2,01}\ ;\quad F_{1/2\ -1/2,00}\ .$$

There are eight independent density matrix elements for K*, therefore, we can write down the relations which must be satisfied when the Pomeron-pole is exchanged. The relations are:

$$\rho_{22} - \rho_{2-2} = 0\ ;$$

$$\rho_{11} + \rho_{1-1} = 0;\quad (1 - \rho_{00}) + 2(\rho_{1-1} - \rho_{2-2}) = 0$$

$$\mathrm{Re}\ \rho_{21} + \mathrm{Re}\ \rho_{2-1} = 0$$

$$\rho_{22}\,\rho_{11} - |\rho_{21}|^2 = 0$$

$$\rho_{22}\,\rho_{00} - |\rho_{20}|^2 = 0$$

$$\rho_{11}\,\rho_{00} - |\rho_{10}|^2 = 0$$

For the Pomeron-cut $P_r = \pm 1$, we get the following restrictions among the density matrix elements and the helicity amplitudes:

$$\rho_{22} - \rho_{2-2} = 4N|F_{1/2\ 1/2,02}|^2$$

$$\rho_{11} + \rho_{1-1} = 4N|F_{1/2\ 1/2,01}|^2$$

$$\mathrm{Re}\ \rho_{21} + \mathrm{Re}\ \rho_{2-1} = 4N|F_{1/2\ 1/2,02}||F_{1/2\ 1/2,01}|\ .$$

The right hand side of each equation becomes zero for $P_r = +1$. Hence, if we plot the left hand side against t for the cut, we get a discontinuous curve. The principal mode of decay of this resonance is πK, and an experimental study of the angular distributions of the decay process is suggested to verify our results. When this data becomes available, this would provide a convenient test on the nature of the Pomeron singularity.

In conclusion, we suggest[36] that the experiments may be carried out on the decay of unstable particles. N*(isospin 1/2), A_1^+, K*(1320) and K*(1790) to check the consistency of our results.

CHAPTER V

Present Status of the Pomeron Trajectory and Conclusion

As is clear from the earlier chapters, the Pomeron trajectory is different, in many respects, from other ordinary trajectories[37]. In this chapter, we briefly report the experimental results on the Pomeron trajectory, its theoretical implications and some aspects of its difficulties to explain the experimental data.

Firstly, one should be able to associate known particleswith each trajectory. The trajectory and the residue functions should also extrapolate smoothly to their value at the pole of the physical particles. The only exception is the Pomeron trajectory, where no known particle can be associated. The lowest particle on this trajectory must have spin 2 and a positive parity. Such a particle was found with mass of 1250 Mev, but the extrapolation from the $\alpha_p(0) = 1$ to the 2^+ particle gave the slope of the Pomeron trajectory as $0.65\ (\text{Gev})^{-2}$. But recent experimental data on pp-scattering at energies greater than 20 Gev/c, gives fits yielding the value of 0.4 for the slope of the Pomeron trajectory. Therefore one has to abandon this particle to lie on the Pomeron trajectory. There is another reason namely that this known particle can fit very well on other ordinary trajectories with the normal slope of $1\ (\text{Gev})^{-2}$.

Other than the slope of the Pomeron trajectory, there are some doubts about the intercept of the Pomeron trajectory. As mentioned in the first chapter, the unit value of the intercept has been used to derive two high energy theorems. Also a recent discussion[38] of the analytic properties of the trajectories and their residues, as the mass

of their first physical occurrence approaches zero, suggests that the small value of the slope is closely tied to the fact that the intercept is unity. But there are also evidences indicating that the intercept is slightly less than unity. A calculation[39] of the shift due to electromagnetic interaction of the intercept, which was assumed to be unity in the absence of such interactions, found $\alpha_p(0) = 0.94$. Another reason is that in order for the residue to obey the algebra of $U(3) \otimes U(3)$, the intercept must be 0.93[40]. This also implies that the total cross-sections must tend to zero at asymptotic energy. The intercept of the Pomeron trajectory has also been determined from an application of continuous moment sum rules[41] to low energy πN total cross-section data to be unity with an uncertainty of 0.02 - 0.03.

The Pomeron has been used in many experimental fits in elastic scattering by many authors[42]. It has been used in P + P' + ρ model to fit total cross-sections for $\pi^{\pm}p$ scattering, and in a P + P' + w model to make a study of the NN and $N\bar{N}$ elastic data. Recently, these two models have been used in a combined study of πp, pp and $p\bar{p}$ elastic scattering data[43]. One notices, that, in general the parameters obtained for the P' trajectory depend on what assumptions are made about those of the Pomeron. For example, Logan and Razmi assume the intercept of the Pomeron to be unity and find $\alpha_{P'}(0) = 0.67$; but if they assume $\alpha_P(0) = 0.93$, they find $\alpha_{P'}(0) = 0.64$ with a proper fit. Hence, the conclusion is that there is still an uncertainty about the exact intercept of the Pomeron trajectory, but the slope is nearly well established from the highest available energy.

There are arguments that the Pomeron singularity can be a fixed pole, or cut or some other essential singularity. As we mentioned in the first chapter, the Pomeron can be exchanged with other trajectories

to produce a cut. If the intercept of the Pomeron is unity, the branch point of the cut will have the same intercept as the other trajectory and a slope less than that of either trajectory. To avoid the accumulation of the branch points of an infinite number of cuts at $J = 1$, it has been suggested that $\alpha_p(0) = 1 - \epsilon$ [44]. The cut mechanism is not sufficient to allow the slope of the Pomeron to be zero and, consequently, it is unlikely that the Pomeron is a fixed pole[45]. Therefore, the Pomeron may represent some other type of singularity.

Few authors have suggested models for cuts, but so far without much success to evaluate its contribution. Qualitatively, to distinguish between a pole and a branch point, one would expect the pole to have a non-zero slope (shrinkage), definite parity and factorization to hold. In the case of the branch point, factorization would fail to some extent, there would not be unique parity, and the effective slope, if non-zero, would be expected to decrease with increasing t.

The present state of the Pomeron trajectory gives more evidence that it is a simple pole. This is the main conclusion of our study in this thesis. Chapter II explains that the factorization is favoured in case of elastic, quasi-two-body reactions, and for reactions in three-particles in the final state. Secondly, Chapter IV also favours that the Pomeron must have a definite parity, though there are lots of predictions that are required to be tested experimentally.

In conclusion, the Pomeron appears to possess pole-like properties, but surely it is an unusual trajectory and we have just begun to understand its role in high energy scattering.

REFERENCES

1. G.N.Watson, Proc. Roy. Soc. 95, 83 (1918).

   A. Sommerfeld, Vorlesungen Uber Theoretische Physik, Vol. VI, p. 282, Leipzig Geestu. Protig 1945.

2. T. Regge, Nuovo Cimento 14, 951 (1959); Nuovo Cimento 18, 947 (1960).

3. G.F.Chew and C.S.Frautschi, Phys. Rev. Lett. 8, 41 (1962).

   V.N.Gribov and I. Ya. Pomeranchuk, Phys. Rev. Lett. 8, 343; 412, (1962).

4. A. Bialas et al., Nuc. Phys. B11, 479 (1969).

5. M. Froissart, Phys. Rev. 123, 1053 (1961).

6. I. Ya. Pomeranchuk, Soviet Phys. JETP 7, 499 (1958).

7. G.G.Beznogikh et al.,Phys. Lett. 30B, 274 (1969).

8. D. Amati, S. Fubini and A. Stranghellini, Nuovo Cimento 26, 896 (1962).

9. P.G.O.Freund, Phys. Rev. Lett. 21, 1375 (1968).

10. S. Mandelstam, Nuovo Cimento 30, 1127 ; 30, 1148 (1963).

11. M.L.Good and W.D.Walker, Phys. Rev. 120, 1857 (1960).

12. J. Bartsch et al.,Nuc. Phys. B19, 381 (1970).

13. L. Van Hove, Some trends and problems in the study of High Multiplicity Hadrons interactions, Colloquium on High Multiplicity Hadronic Interactions, Paris, 13-15 May, 1970, CERN TH1178.

14. W. Kittle et al., "Single and double dissociation in πp collisions" Paper submitted to the XVth International Conference on High Energy Physics", Kiev, 26 August - 4 September, 1970.

15. M.B.Bari, M.S.K.Razmi, Phys. Rev. D2, 9, 2054 (1970).

16. H. Boggild et al., Phys. Lett. 30B, 369, (1969).

17. K.J.Foley et al., Phys. Rev. Lett. 19, 397 (1967).

18. S.J.Lindenbaum et al., Phys. Rev. Lett. 11, 425 (1963).

19. E.W.Anderson et al., Phys. Rev. Lett. 25, 699 (1970).

20. F. Arbab and R.C.Brower, Phys. Rev. 175, 1991 (1968).

W. Rarita, R.J.Riddell, C.B.Chiu and R.N.J.Phillips, Phys. Rev. 165, 1615 (1968).

21. G. Hohler and R. Strauss, "On the determination of the ρ-meson Regge pole parameters" Karlsruhe University preprint.

22. Orsay-Bari-Bologna-Florence Group contribution to Topical Conference on High Energy Collision of Hadrons, CERN, 68-7 Vol. I, p. 106.

23. P. Sonderegger et al., Phys. Lett. 20, 79 (1966).

24. D. Brown, et al., Phys. Rev. Lett. 19, 664 (1967).

25. V.N.Gribov, Yad. Fiz. 5, 197 (1967) (Soviet Journal of Nuclear Physics 5, 138 (1967)).

26. D.R.O.Morrison, Phys. Rev. 165, 1699 (1968).

27. M. Jacob and G.C.Wick, Ann. Phy. (N.Y.) 7, 404 (1959).

28. M. Andrews and J. Gunson, J. Math. Phys. 5, 1391 (1964).

29. F. Calogero, J.M.Charap and E.J.Squires, Ann. Phys. (N.Y.) 25, 825 (1963).

30. T.L.Trueman and G.C.Wick, Ann. Phys. (N.Y.) 26, 322 (1964).

31. R.L.Thews, Phys. Rev. 155, 1624 (1967).

32. K. Gottfried and G.D.Jackson, Nuovo Cimento 33, 309 (1964).

33. G.A.Ringland and R.L.Thews, Phys. Rev. 170, 1569 (1968).

34. E.W.Anderson, et al., Phys. Rev. Lett. 16, 588 (1966).

35. E.W.Anderson et al., Phys. Rev. Lett. 25, 699 (1970).

36. M.B.Bari and K. Ahmed, University of Tabriz preprint, H.E.G./TU/71/3.

37. M.A.Alam, M.B.Bari, F. Nami, University of Tabriz preprint, H.E.G./TU/71/6 (to be published in Nuovo Cimento Lett.)

38. R. Omnes, Phys. Rev. 168, 1893 (1968).

39. F. Buccella et al., Nuovo Cimento 55A, 27 (1968).

40. L.P.Horowitz and H. Neumann, Phys. Rev. Lett. 19, 765 (1967).

41. F. Arbab and R.C.Brower, Phys. Rev. 175, 1991 (1968).

42. C.B.Chiu, S. Chu and L. Wang, Phys. Rev. 161, 1568 (1967).
See also the review article of J.D.Jackson, Revs. of Modern Phys. Vol. 42, No. 1 (1970).

43. W. Rarita, et al., Phys. Rev. 165, 1615 (1968).

44. Y. Srivastava, Phys. Rev. Lett. 19, 47 (1967).

45. J. Finkelstein and K. Kajantie, Phys. Lett. 26B, 305 (1968).

GRAPH CAPTIONS

Graph 1 The graph of $< \rho_{1-1} >$ against t in the reaction $NN \to NN^*(1400)$ for the Pomeranchukon pole exchange in the t-channel.

Graph 2 The graph of ρ_{33}, Re ρ_{31}, Re ρ_{3-1} against t in the reaction $NN \to NN^*(1520)$ for the Pomeranchukon pole exchange in the t-channel.

Graph 3 The graph of $< \rho_{1-1} >$ against t in the reaction $\pi N \to \pi N^*(1400)$ for the Pomeranchukon pole exchange in the t-channel.

Graph 4 The graph of density matrix elements in $\pi N \to \pi N^*(1690)$ for the elements ρ_{55}, ρ_{51}, ρ_{5-1} of the Pomeranchukon pole exchange in the t-channel.

Graph 5 The graph of density matrix elements in $\pi N \to \pi N^*(1690)$ for the elements ρ_{5-3}, ρ_{33}, ρ_{1-1} of the Pomeranchukon pole exchange in the t-channel.

Graph 6 The graph of density matrix elements in $\pi N \to \pi N^*(1690)$ for the elements ρ_{53}, ρ_{31} of the Pomeranchukon pole exchange in the t-channel.

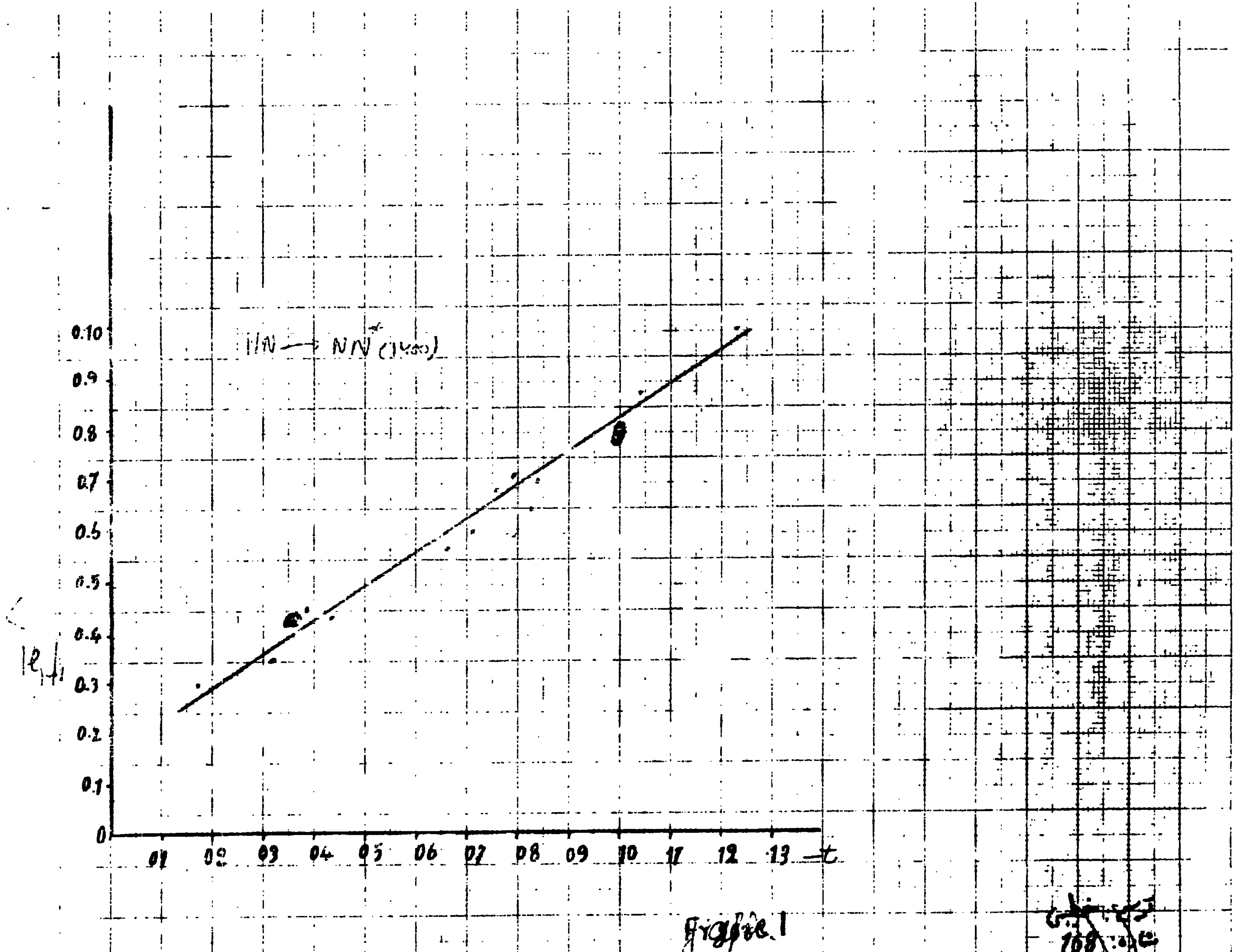

$|\ell_{i+1}|$
0.10
0.9
0.8
0.7
0.5
0.5
0.4
0.3
0.2
0.1
0
01 02 03 04 05 06 07 08 09 10 11 12 13
t

graph I

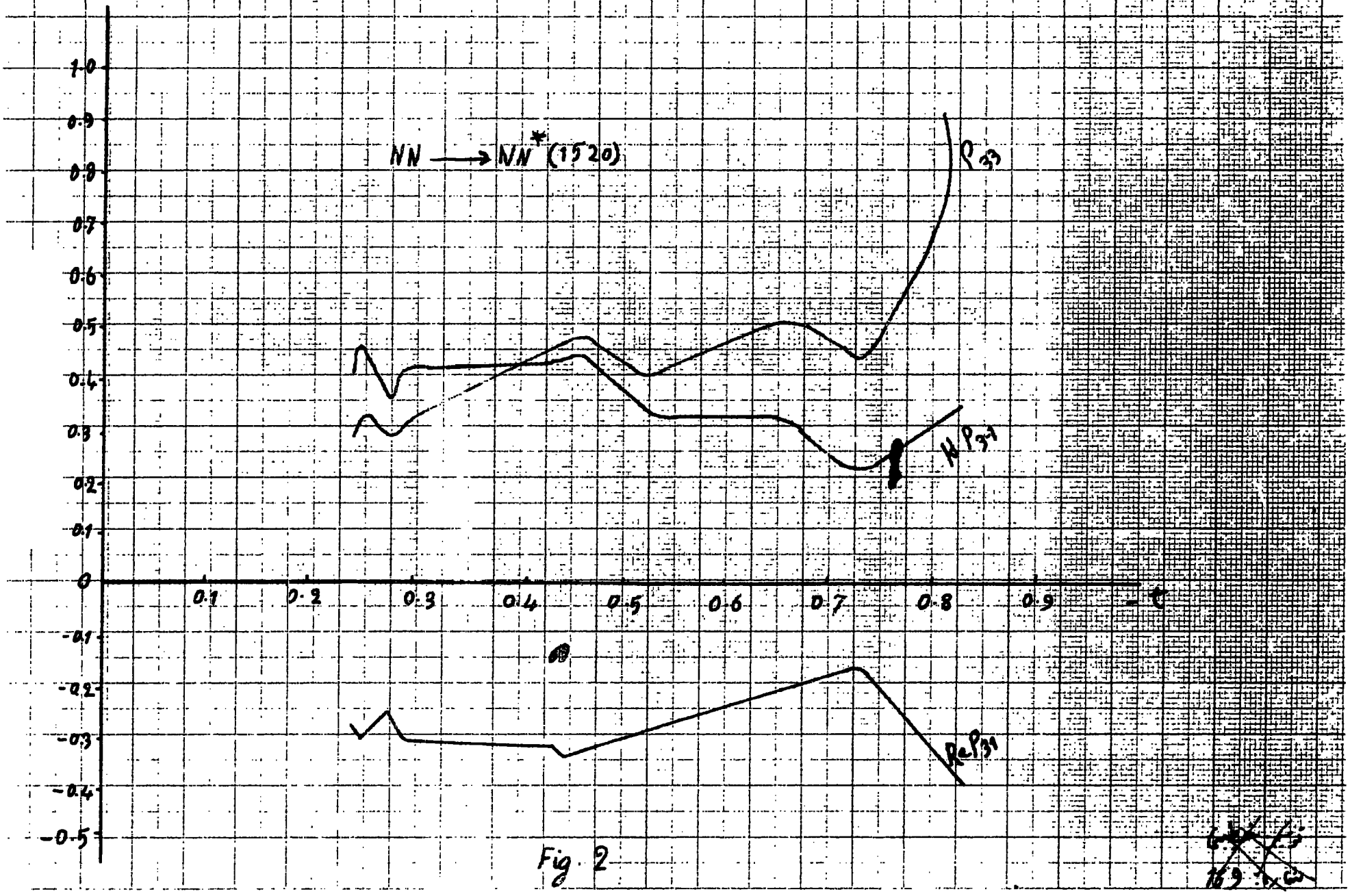

Fig. 2

graph II

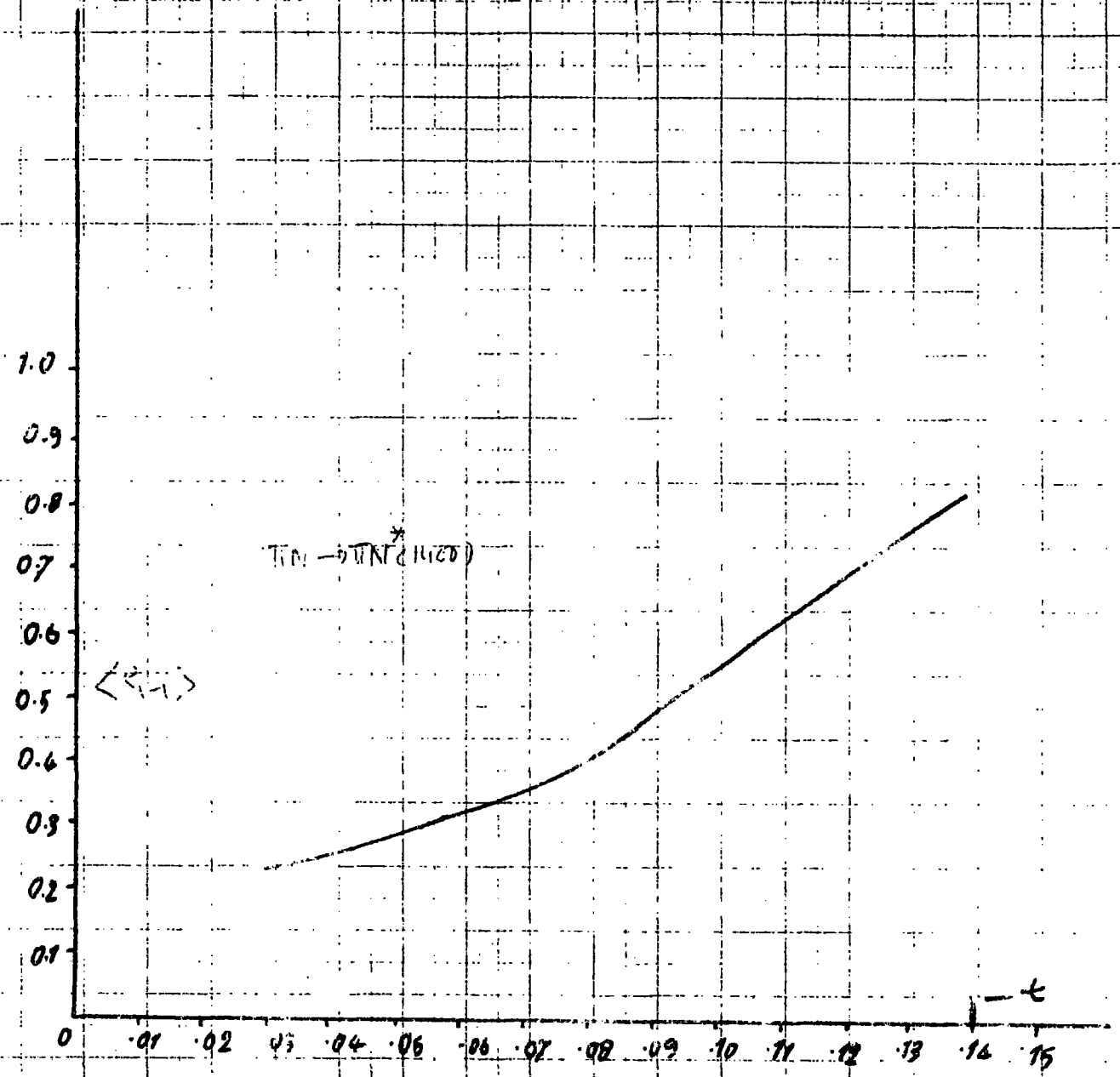

Fig: 23

graph III

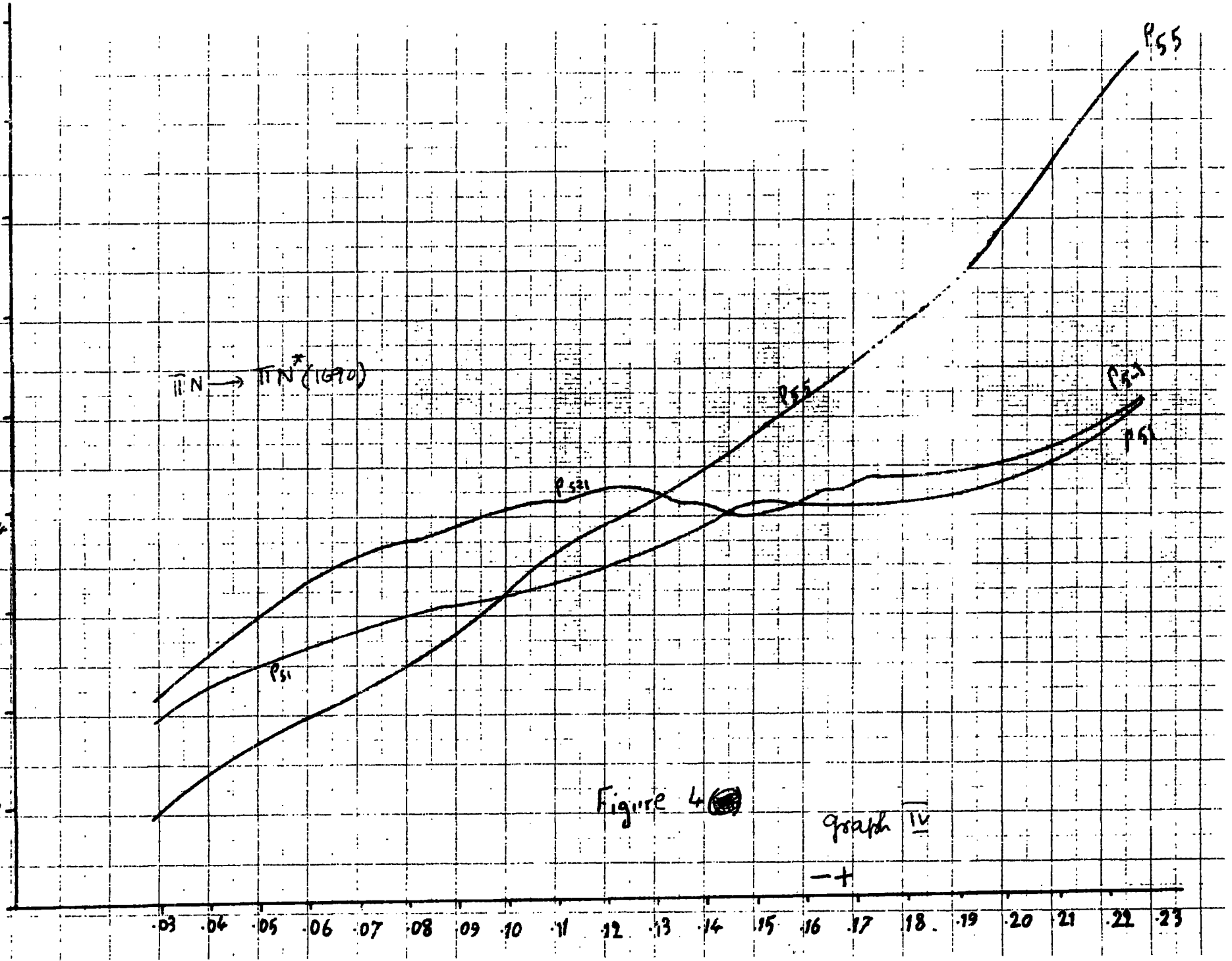
0.9
0.8
0.7
0.6
0.5
0.4
0.3
0.2
0.1
.03 .04 .05 .06 .07 .08 .09 .10 .11 .12 .13 .14 .15 .16 .17 .18 .19 .20 .21 .22 .23
$\bar{\Pi} N \rightarrow \Pi N^*(1690)$
ρ_{55}
ρ_{55}
ρ_{51}
ρ_{531}
ρ_{51}
graph IV
−+

Figure 4

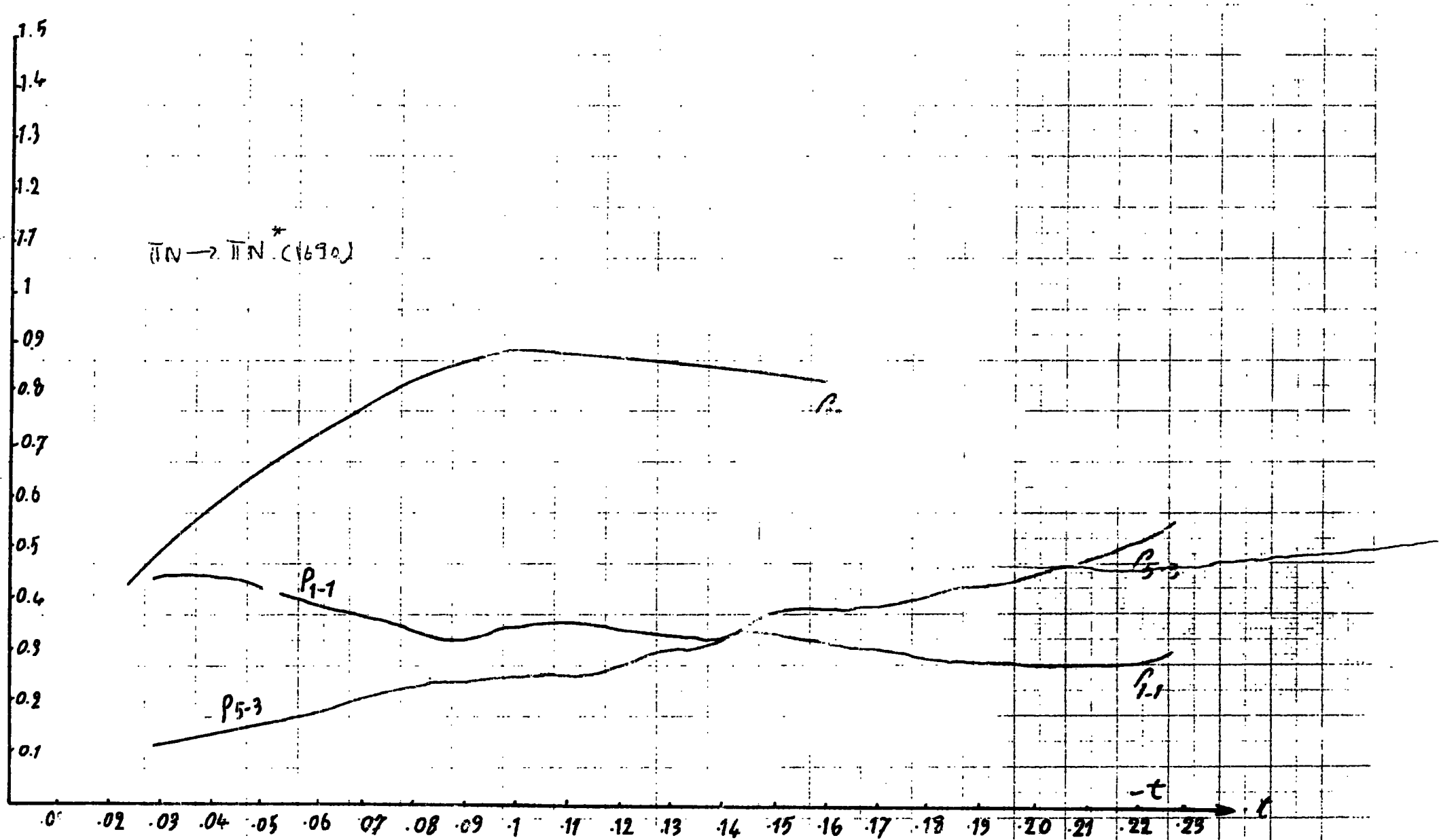

Figure (5)

graph V

165 : ص

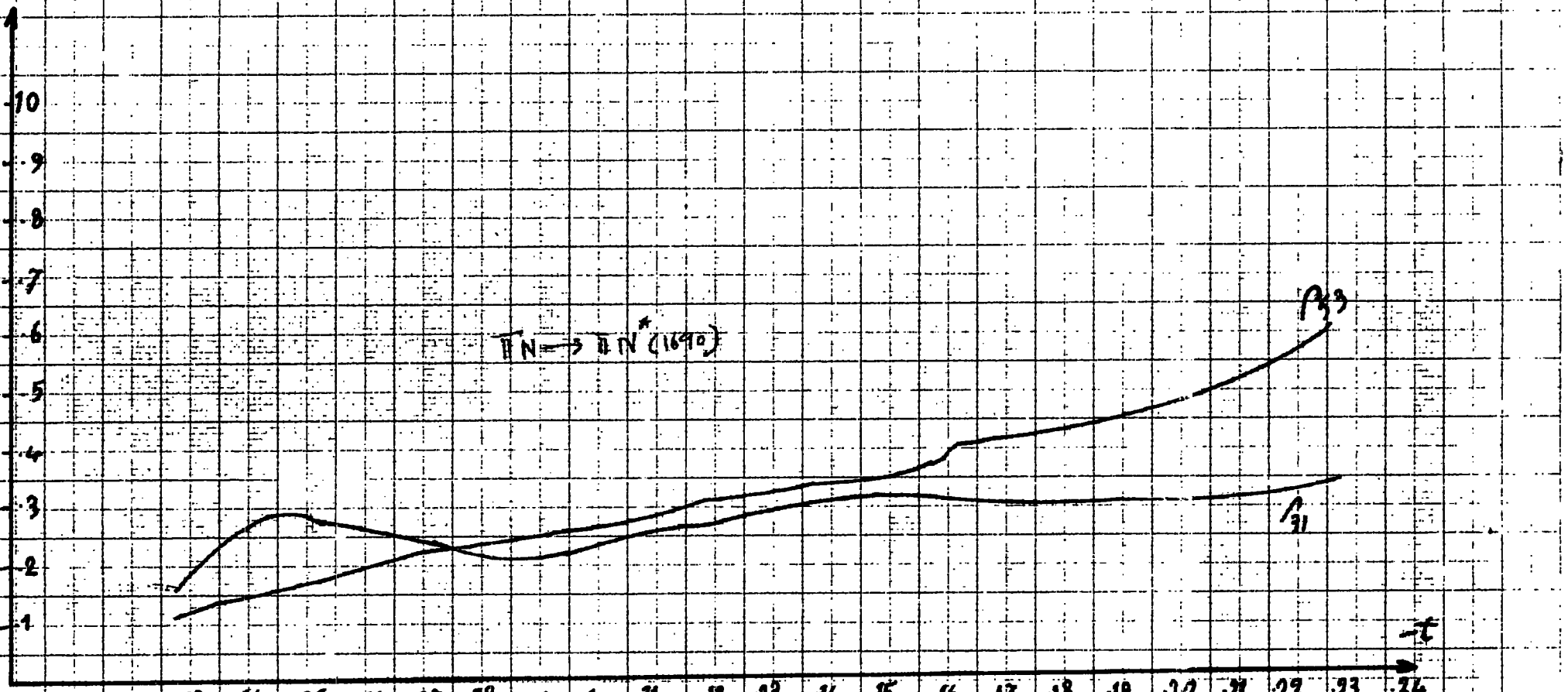

Figure 4 (a)

graph N°1

توسیع خطی

شارہ: 166